NASA Contractor Report 165607

NUMERICAL SIMULATION OF ONE-DIMENSIONAL HEAT TRANSFER IN COMPOSITE BODIES WITH PHASE CHANGE

Kenneth J. DeWitt and Gurudutt Baliga

University of Toledo
Toledo, Ohio 43606

March 1982

Prepared for

NATIONAL AERONAUTICS AND SPACE ADMINISTRATION
Lewis Research Center
Under Grant NAG3-72

TABLE OF CONTENTS

NOMENCLATURE

C	specific heat (Btu/lb°F)
h	heat transfer coefficient (Btu/hr ft^2 °F)
k	thermal conductivity (Btu/hr ft °F)
L	slab thickness (ft)
q	volumetric heat source (Btu/hr ft^3)
q"	heat source per unit area (Btu/hr ft^2 or Watts/in^2)
T	temperature (°F)
x	space direction (in)
$\overline{X}$	dimensionless space direction

Greek Letters

α	thermal diffusivity (ft^2/hr)
Δt	size of time step (sec)
ΔT	temperature semi-interval across T_f (°F)
Δx	grid spacing in x direction (in)
$\Delta \overline{X}$	dimensionless grid spacing in x direction
$\Delta \theta$	dimensionless temperature semi-interval across θ_f
θ	dimensionless temperature
λ	latent heat of ice (Btu/ft^3)
ρ	density (lb/ft^3)

Subscripts

j	layer in the composite body
i	grid point
s	solid or ice region

w	liquid or water region
f	phase change
o	ambient at lower boundary of composite body
∞	ambient at upper boundary of composite body

Superscripts

n	time step
*	ice-water "mushy" region

I. INTRODUCTION

The formation of ice on aircraft components, a wing section of which is shown in Figure 1, poses tremendous difficulties in aircraft operation. Various anti-icing and de-icing methods have been investigated and are reported in Reference (1). Before these methods are considered, it is necessary to differentiate between anti-icing and de-icing. The anti-icing principle involves methods to prevent ice formation on the blade surface. These methods usually require an excessive amount of energy and are not frequently applied. The de-icing principle involves shedding the ice by heating the surface on which it is formed. In this case the energy required is reduced significantly because heat is needed only to form a thin water film between the aircraft structure and the ice, thereby decreasing the adhesion strength and allowing the aerodynamic forces to sweep away the ice layer.

At present, for anti-icing and de-icing, thermal energy is the most commonly used technique and is obtained in two ways:

(i) Electrical resistance heating elements which are embedded just below the surface being heated (as shown in Figure 1);

(ii) Passing hot, engine compressed bleed air through passages below the surface being heated.

A. TYPES OF DE-ICING AND ANTI-ICING SYSTEMS

Various de-icing and anti-icing techniques have been developed over the years, some of which have been in use for a long time and are listed below.

1. Inflatable Rubber Pneumatic Boots: This pneumatically operated mechanical de-icing system consists of a boot which is made of a flexible rubber-like material, and which is slipped over the wing of the aircraft such that the ice forms on the boot-surface rather than on the wing structure. The boots, when inflated with the cooled engine bleed air, break the ice surface, thus allowing the aerodynamic forces to blow the ice away. A section of the aircraft wing fitted with a boot is shown in Figure 2. This method is relatively simple and uses a very small quantity of the cooled engine bleed air and does not impose any fuel penalty on the engine. However, because the surface of the boot is not as smooth as the wing surface, the boot system increases the drag for the aircraft. In addition, this pneumatic de-icer system requires frequent maintenance and replacement. For the pneumatic boots to show an operational weight advantage over the thermal de-icing system technique, they must be virtually drag-free. Modern boots, carefully bonded to the wing structure, do minimize the drag but are expensive to maintain.

2. Chemical Systems: An anti-icing method used to prevent the formation of ice on the abrasion shield surface of the aircraft involves the use of freezing point depressants. The chemical depressants are spread in a thin film over the abrasion shield, thus lowering the water freezing point and preventing the formation of ice. Though relatively simple in concept, their usefulness is restricted because of the variable external pressure field, which makes it difficult to obtain a uniform flow distribution of the depressants, and which therefore can result in the formation of ice on the unprotected areas. Further drawbacks are that the systems require frequent resupply and are sensitive to clogging of the fluid distribution holes in dusty environments. Chemical systems are therefore restricted in their use to mainly windshield ice protection.

3. Thermal De-icing: Thermal de-icing remains the most commonly used technique in removing the ice from the abrasion shield surface. In this method the ice covered regions are cyclically heated in sequence either by electric heaters or by hot bleed air from the engine. The thermal energy supplied is used to raise the temperature of the surface on which the ice is deposited to 32°F and to melt a thin layer of ice. This thin film of water reduces the adhesion strength of the ice to the surface and aerodynamic forces then sweep the unmelted ice from the surface. Because of the cyclical nature of the energy input, the energy

requirement is very much less compared to the other techniques. In addition, the use of this system is not restricted due to change in weather conditions and is relatively easy to maintain.

Of the above mentioned systems, the electro-thermal de-icing technique is the most commonly used and will be the one considered in this study.

B. DE-ICING PAD CONFIGURATION

The configuration of the electro-thermal de-icing pad is shown in Figure 1. It is essentially a composite body consisting of five layers in the case of a point heat source and six layers in the presence of a finite heater. The heating source is separated from the metal substrate, or the aircraft blade, by the inner insulation which usually consists of resin impregnated glass cloth. This insulation serves to provide electrical insulation for the heating element, and also directs the heat towards the ice layer. It is advantageous to have a large ratio of inner to outer insulation thickness so that more heat flows toward the ice layer, thereby reducing the de-icing time. The heater element usually consists either of a woven mat of wires and glass fibers or of multiple strips of resistance ribbon.

In order to protect the de-icer pad from rain erosion or sand and stone abrasion, which could be a problem while flying at high speeds, an abrasion shield, frequently made of stainless steel, is added to the outer insulation. The

abrasion shield also serves to diffuse the heat from the heater, thus providing more uniform heating and thereby reducing cold spots where ice could form above the gaps in the heater elements.

The material of construction of the substrate depends on the type of aircraft and is most often an aluminum alloy.

In this study, only the one-dimensional model of the de-icing pad will be investigated. It is assumed that there is perfect adhesion between each of the layers and therefore no contact resistance to heat flow will be considered in this analysis. This study will concern itself with both a point heat source and a finite thickness heater, providing either constant or time dependent heat output. In each of these cases, the effects of the type and thickness of the insulation layers and the nature of the blade structure on the de-icing time will be observed. In the first section of this study, the phase change at the ice-abrasion shield interface will not be considered and the ice layer will be treated as a single phase. In the latter part, for the ice-water phase change, a numerical method which approximates the latent heat effect by a large heat capacity over a small temperature interval will be applied.

II. LITERATURE REVIEW

From the conducted literature review, it is evident that the de-icing problem has either been ignored or that information pertaining to it has not been published in the open literature. Of the few attempts that have been made to solve the specific problem, Wardlaw(2) and Campbell(3) applied an analytical approach, while Stallabrass(4) has made use of a numerical technique. However, several methods have been proposed to solve the transient heat conduction problem in a composite slab, without phase change and with different boundary conditions, and these will be reviewed below.

A. ANALYTICAL TECHNIQUES FOR COMPOSITE BODY HEAT TRANSFER

The Laplace transformation technique was presented by Carslaw and Jaeger(5), but this method becomes increasingly tedious to apply to composite bodies with more than two layers since it becomes more difficult to obtain the inverse Laplace transform. Goodman(6) introduced the method of the adjoint solution, which arises from consideration of an auxiliary function. However, a disadvantage of the adjoint method is that the solution provides just the interfacial temperatures and not the temperature profile within each slab layer. Further work on the adjoint solution method has

been done by Bouchillon(7) in which transient cases have been considered. The formulated integral equations have been reduced to linear equations and then solved by matrix inversion techniques. However, as before, only the interfacial temperatures can be calculated.

The Orthogonal-Expansion technique proposed by Tittle (8,9) is another method to solve the boundary-value heat conduction problem in multilayer regions. The method is basically an extension of the Sturm-Liouville problem to the case of a one-dimensional multilayer region. Orthogonal sets are constructed from the solution of each of the layers and an orthogonality factor, called the discontinuous weighting function, is used such that the resulting orthogonal set is applicable to the entire composite media.

Bulavin and Kashcheev(10) used the method of separation of variables and of orthogonal expansion of functions over a one-dimensional multilayer region to solve the transient heat conduction problem involving heat sources in a multilayer region. Campbell(3) applied a similar method in solving the de-icer pad problem analytically.

The disadvantage of using an analytical technique is that for each temperature desired, an excessive amount of calculations have to be performed. Hence, as the number of layers within the body increases, the calculations become more tedious. This drawback can be overcome by using numerical techniques.

B. NUMERICAL TECHNIQUES FOR COMPOSITE BODY HEAT TRANSFER

The most frequently used numerical method for solving partial differential equations is the finite-difference method. Using this method, the temperature at all the nodal points within the composite slab can be calculated at each time step. The finite-difference method involves the construction of a grid within the boundary over which the differential problem is to be solved. At each of the grid points the differential operators are replaced by their approximate values expressed in terms of functions. This substitution reduces the problem to the solution of a set of algebraic equations, which is mathematically easier to solve. A finite-difference representation of the de-icer pad is shown in Figure 3.

Two of the major considerations in using a finite-difference scheme are the establishment of both a convergence criteria and a stability criteria. A number of finite-differencing methods have been proposed and are discussed in depth in References (11) and (12). In addition, Price and Slack(13) have evaluated the accuracy and stability criteria of various finite-differencing methods for the heat flow equation with convective boundary conditions.

The Crank-Nicolson implicit finite-difference scheme is unconditionally stable for all time steps, and has been used in the present study. For the corresponding explicit formulation, there exists a limitation on the ratio $\Delta t/(\Delta x)^2$

to be $0 \leq \Delta t/(\Delta x)^2 \leq 1/2$; no such conditions are present for the implicit scheme. However, the choice of the size of the time and space steps has a direct effect on the accuracy of the solution. The truncation error for the implicit Crank-Nicolson scheme is of the order $(\Delta x)^2$ for the space differential and $(\Delta t)^2$ for the time differential. As stated by Dusinberre(14), the accuracy of the solution can be increased by initially choosing a very small time step and then subsequently increasing it.

Stallabrass(4) employed the explicit finite-difference scheme in his de-icer analysis. Though the scope of his study covers most of the important aspects for the one-dimensional de-icer design, its major drawback is that it considers no phase change within the ice layer and limits the solution to the time at which the interfacial temperature between the ice and the abrasion shield reaches 32°F. Also, Stallabrass(4) considers only a point source and a finite thickness heater with constant heat output. The present study will consider the phase change effect in the ice-layer as well as time varying heat sources.

C. METHODS TO DESCRIBE PHASE CHANGE

Phase change or moving boundary problems have been relatively difficult to solve because of the non-linear nature of the boundary conditions arising from the boundary movement. Various methods of analysis such as the Integral method (15), Successive-Approximation technique (16) and

Series Solution (17) have been proposed for analytically solving the one-dimensional phase change problem. Mori and Araki(18) have reviewed some of the other methods that have been proposed.

Numerical methods to solve the phase change problem have been attempted and are described by Meuhlbauer and Sunderland(19) and Rubinstein(20). Most of the numerical methods solve the pertinent heat conduction equations and determine the temperature distribution in both media, while at the same time locating the position of the solid-liquid interface by a predictor-corrector technique. However, this requires a large number of iterations to locate the solid-liquid interface position at any given time. Mastanaiah(21) used such an iterative scheme with a two time level implicit method for the one-dimensional freezing and melting problem with convective boundary conditions and variable thermal properties. Lazaridis(22) used another iterative solution for the two-dimensional solidification problem with constant thermal properties and convective boundary conditions, and also constant temperature conditions at the boundaries. Crank(23) describes two additional ways to approach the moving boundary problem. The first involves the rearranging of variables such that the boundary is treated as stationary and the problem is transformed into an eigenvalue problem with fixed boundaries. However, the equations to be solved contain parameters associated with the moving boundary

problem for which values have to be determined to satisfy the boundary conditions. In the second method, Lagrangian interpolation formulae for non-equal intervals are introduced along with the finite-difference formulae in order to follow the movement of the boundary.

To avoid the problem of locating the interface position as in the above method, a second approach, the method of weak solution, often called the Enthalpy Method, has been used. In this method, the enthalpy is used as a dependent variable along with the temperature. Thus the moving boundary problem can be solved in a fixed region and no modification is required to satisfy conditions at the moving boundary. Much of the numerical work applying the enthalpy approach to the phase change (Stefan) problems has been done using the finite-difference scheme. Atthey(24) has solved the welding problem in one-dimension, which is essentially a melting problem, using this approach. The convergence criteria for such a solution has also been clearly indicated. The latent heat has, however, been assumed to be evolved at the phase change temperature. In practice, the latent heat is usually considered to be evolved over a small temperature range, ΔT.

Goodrich(25) and Bonacina et al.(26) have solved the one-dimensional ice-water problem by associating the latent heat effect with a finite temperature interval about the phase change isotherm. However, it should be noted that

within this "mushy" region, the grid spacing has to be substantially reduced or else the isotherm may advance in an oscillatory fashion and distort the temperature profile. Goodrich(25) used the Crank-Nicolson implicit finite-difference scheme for formulating the problem and the Gaussian Elimination technique for solving the resulting set of equations. Bonacina et al.(26) used a three-time level implicit scheme for formulating the problem, which was then solved as before. The formulation results in three governing equations applicable to the three phase regions: solid, "mushy" and liquid regions, respectively. The "mushy" region was defined over a small finite temperature range, $2\Delta T$, about the phase change temperature, T_f. The phase change initially starts occurring at temperature $T_f - \Delta T$, and the ice becomes pure liquid at temperature $T_f + \Delta T$, where T_f equals 32°F. The choice of the temperature interval, $2\Delta T$, depends on the physical nature of the problem. For the ice-water system considered in Reference (26), a temperature interval of two degrees Kelvin was assumed and good comparison to the analytical solution was obtained. In the solid and liquid regions the thermal properties were assumed constant. In the "mushy" region, the thermal conductivity was assumed to vary linearly with temperature and the latent heat effect was approximated by a large heat capacity. Solutions to phase change problems applying this method agree fairly accurately with analytical results and this method will therefore be used in the present study.

The enthalpy method has also been employed for solving two-dimensional phase change problems. Meyers(27) and Shamsunder and Sparrow(28) have described a purely implicit two-dimensional finite-difference scheme for solving such problems. Shamsunder and Sparrow(28) have also considered the effect of various parameters on the solidification rate. A finite element approach has been proposed by Comini et al. (29) for solution of the Stefan problem in two-dimensions with non-linear radiation boundary conditions.

The complete numerical formulation of the de-icer problem is given in the next section.

III. NUMERICAL FORMULATION

A. GOVERNING EQUATIONS AND BOUNDARY CONDITIONS

In the formulation for the one-dimensional, unsteady state, mathematical model for the heat transfer analysis of a composite aircraft blade with an ice layer, as shown in Figure 1, the following assumptions were made:

(1) The thermal properties of the material composing each layer of the blade are constant;

(2) Density variations are neglected, as are the effects of the volume contraction experienced when the ice melts;

(3) The individual layers are in perfect contact with each other, and there is no additional resistance present at the interface; and

(4) The ambient temperature is constant.

With the above assumptions the governing equation is

$$\rho_j C_j \frac{\partial T_j}{\partial t} = k_j \frac{\partial^2 T_j}{\partial x^2} + q_j \qquad (1)$$

where j represents the layer in question, ρ, C, k, T and q are the density, heat capacity, thermal conductivity, temperature and volumetric heat source of the j^{th} layer, respectively, and x and t are the distance coordinate and time variable.

The total blade is then characterized by:

j = 1	Blade or Substrate	$q_1 = 0$
j = 2	Lower or Inner Insulation	$q_2 = 0$
j = 3	Heater	$q_3 = f(t)$ (2)
j = 4	Upper or Outer Insulation	$q_4 = 0$
j = 5	Abrasion Shield	$q_5 = 0$

For the ice layer (j=6), the governing equations to be applied depend upon the temperature profile within the layer. Applying the method discussed at the end of Chapter II, References (25,26), the governing equations are:

For j = 6,

Ice: $$\rho_s C_s \frac{\partial T_j}{\partial t} = k_s \frac{\partial^2 T_j}{\partial x^2} \quad , T_j < T_f - \Delta T$$

Water: $$\rho_w C_w \frac{\partial T_j}{\partial t} = k_w \frac{\partial^2 T_j}{\partial x^2} \quad , T_j > T_f + \Delta T \qquad (3)$$

Ice-Water: $$C^* \frac{\partial T_j}{\partial t} = \frac{\partial}{\partial x}\left[k^* \frac{\partial T_j}{\partial x}\right] \quad T_f - \Delta T \leq T_j \leq T_f + \Delta T$$

where $$C^* = \frac{\lambda}{2\Delta T} + \frac{\rho_s C_s + \rho_w C_w}{2}$$

$$k^* = k_s + \frac{k_w - k_s}{2\Delta T}\left(T_j - \left(T_f - \Delta T\right)\right)$$

In the above equations, C_s and C_w, ρ_s and ρ_w and k_s and k_w are the specific heats, densities and thermal conductivities of ice and water, respectively. The latent heat λ, is assumed to be evolved over the fictitious temperature interval $2\Delta T$ (2°F in this study). The phase change initially starts occurring at temperature $T_f - \Delta T$ and the ice becomes

pure liquid at temperature $T_f + \Delta T$, where T_f equals 32°F. Within the temperature range $T_f - \Delta T$ and $T_f + \Delta T$, a single phase does not exist and the ice-water system is said to be in the "mushy" region. As discussed previously, a large heat capacity to account for the latent heat and a linearized thermal conductivity are used to describe this "mushy" region. The thermal properties in the ice and water regions are assumed to remain constant.

The corresponding boundary conditions to be used are:

(i) The equality of the temperatures and heat fluxes at the interfacial points:

$$\left.T_j\right|_I = \left.T_{j+1}\right|_I \qquad j = 1,\ldots,5$$
$$-k_j \left.\frac{\partial T_j}{\partial x}\right|_I = -k_{j+1} \left.\frac{\partial T_{j+1}}{\partial x}\right|_I \qquad j = 1,\ldots,5 \tag{4}$$

where the subscript I denotes the interface;

(ii) Convective heat transfer at the lower and upper boundaries:

$$k_j \left.\frac{\partial T_j}{\partial x}\right|_{x=0} = h_1\left(\left.T_j\right|_{x=0} - T_0\right) \quad , j = 1 \tag{5a}$$

$$-\bar{k}_j \left.\frac{\partial T_j}{\partial x}\right|_{x=L} = h_2\left(\left.T_j\right|_{x=L} - T_\infty\right) \quad , j = 6 \tag{5b}$$

where

$$\bar{k}_j = k_s \quad \text{for} \quad \left.T_j\right|_{x=L} < T_f - \Delta T$$
$$\bar{k}_j = k_\omega \quad \text{for} \quad \left.T_j\right|_{x=L} > T_f + \Delta T$$
$$\bar{k}_j = k^* \quad \text{for} \quad T_f - \Delta T \leq \left.T_j\right|_{x=L} \leq T_f + \Delta T$$

To formulate the above equations in terms of non-dimensional temperature and distance, the following definitions are made:

$$\Theta = \frac{T}{T_{ref}} \qquad \bar{X} = \frac{X}{L} \qquad \alpha_j = \frac{k_j}{\rho_j C_j} \tag{1'}$$

where T_{ref} = the reference temperature (taken to be 32°F in this study),

L = the total length of the composite slab, and

α_j = the thermal diffusivity of the j^{th} layer.

Substitution of the above dimensionless quantities into equations (1) through (5) yields

$$\frac{\partial \theta_j}{\partial t} = \frac{\alpha_j}{L^2}\frac{\partial^2 \theta_j}{\partial \bar{X}^2} + \frac{q_j}{T_{ref}\rho_j C_j} \quad , j = 1,\ldots,5 \tag{2'}$$

For j = 6

Ice: $$\frac{\partial \theta_j}{\partial t} = \frac{\alpha_s}{L^2}\frac{\partial^2 \theta_j}{\partial \bar{X}^2} \qquad \theta_j < \theta_f - \Delta\theta$$

Water: $$\frac{\partial \theta_j}{\partial t} = \frac{\alpha_w}{L^2}\frac{\partial^2 \theta_j}{\partial \bar{X}^2} \qquad \theta_j > \theta_f + \Delta\theta \tag{3'}$$

Ice-water: $$L^2 C^* \frac{\partial \theta_j}{\partial t} = \frac{\partial}{\partial \bar{X}}\left[k^* \frac{\partial \theta_j}{\partial \bar{X}}\right] \qquad \theta_f - \Delta\theta \le \theta_j \le \theta_f + \Delta\theta$$

where $$C^* = \frac{\lambda}{2 T_{ref} \Delta\theta} + \frac{\rho_s C_s + \rho_w C_w}{2}$$

$$k^* = k_s + \frac{k_w - k_s}{2\Delta\theta}\left(\theta_j - (\theta_f - \Delta\theta)\right)$$

At the interfacial points,

$$\theta_j\big|_I = \theta_{j+1}\big|_I \qquad j = 1,\ldots,5$$

$$-k_j \frac{\partial \theta_j}{\partial \bar{X}}\Big|_I = -k_{j+1} \frac{\partial \theta_{j+1}}{\partial \bar{X}}\Big|_I \qquad j = 1,\ldots,5 \tag{4'}$$

Finally, at the lower and upper boundaries:

at $\bar{X} = 0$, $j = 1$

$$k_j \frac{\partial \theta_j}{\partial \bar{X}}\Big|_{\bar{X}=0} = h_1 L \left(\theta_j\big|_{\bar{X}=0} - \theta_o\right) \tag{5a'}$$

at $\bar{X} = 1$, $j = 6$

$$-\bar{k}_j \frac{\partial \theta_j}{\partial \bar{X}}\Big|_{\bar{X}=1} = h_2 L \left(\theta_j\big|_{\bar{X}=1} - \theta_\infty\right) \tag{5b'}$$

where

$$\bar{k}_j = k_s \quad \text{for} \quad \theta_j\big|_{\bar{X}=1} < \theta_f - \Delta\theta$$

$$\bar{k}_j = k_w \quad \text{for} \quad \theta_j\big|_{\bar{X}=1} > \theta_f + \Delta\theta$$

$$\bar{k}_j = k^* \quad \text{for} \quad \theta_f - \Delta\theta \leq \theta_j\big|_{\bar{X}=1} \leq \theta_f + \Delta\theta$$

The above equations can now be represented in finite-difference form and solved numerically.

B. NUMERICAL TECHNIQUE

In the numerical solution of the above partial differential equations, a finite-difference scheme was adopted. This is accomplished by constructing a system of grid points which define a finite number of regularly spaced values of

the dependent variable, in this case the temperature, over the whole space domain at each time step. As illustrated in Figure 3, the X-axis represents the length along the composite body and the Y-axis represents the time variable. The space axis is divided into increments of size $\Delta\bar{X}_j$, where the subscript j indicates the layer in question. Within each layer, the space increment $\Delta\bar{X}_j$ is constant, but it may vary from one layer to the next. The time axis is divided into equal time step intervals, Δt. However, the time increment may be increased as the solution progresses. The index i denotes the position of the variable in the grid along the space axis, and the superscript n indicates the value of the variable at time n. Hence the quantity $\theta^{n}_{j,i}$ represents the non-dimensional temperature in the j^{th} layer, at position i along the space axis, at time n.

C. FINITE-DIFFERENCING AND THE METHOD OF SOLUTION

The finite-difference approximation to a partial derivative can be derived using a Taylor Series expansion around any grid point. In this study, the Crank-Nicolson Implicit scheme was applied in order to maintain stability of the solution. The finite-difference approximations for the first and second-order space derivatives and first order time derivative are second order correct and are given below.

$$\left.\frac{\partial \theta_j}{\partial \bar{X}}\right|_i^{n+1/2} = \frac{\theta^{n+1}_{j,i+1} - \theta^{n+1}_{j,i-1} + \theta^{n}_{j,i+1} - \theta^{n}_{j,i-1}}{4\Delta\bar{X}_j} + O(\Delta\bar{X}_j)^2 \qquad (6a)$$

$$\left.\frac{\partial^2\theta_j}{\partial \bar{X}^2}\right|_i^{n+1/2} = \frac{\theta_{j,i+1}^{n+1} - 2\theta_{j,i}^{n+1} + \theta_{j,i-1}^{n+1} + \theta_{j,i+1}^{n} - 2\theta_{j,i}^{n} + \theta_{j,i-1}^{n}}{2(\Delta\bar{X}_j)^2} + O(\Delta\bar{X}_j)^2 \tag{6b}$$

$$\left.\frac{\partial\theta_j}{\partial t}\right|_i^{n+1/2} = \frac{\theta_{j,i}^{n+1} - \theta_{j,i}^{n}}{\Delta t} + O(\Delta t)^2 \tag{6c}$$

In the above equations the superscripts represent the time levels n and n+1, the subscript j represents the j^{th} layer and the subscript i represents the grid point under consideration.

The Crank-Nicolson finite-difference equations are obtained by substituting (6a,b,c) into equations (2') through (5'). The governing equations in finite-difference form reduce to:

$$\theta_{j,i-1}^{n+1} - 2\left(1 + \frac{(L\Delta\bar{X}_j)^2}{\alpha_j \Delta t}\right)\theta_{j,i}^{n+1} + \theta_{j,i+1}^{n+1} = -\theta_{j,i-1}^{n} - \frac{2(L\Delta\bar{X}_j)}{T_{ref}\, k_j} q''_j - \theta_{j,i+1}^{n} + 2\left(1 - \frac{(L\Delta\bar{X}_j)^2}{\alpha_j \Delta t}\right)\theta_{j,i}^{n} \tag{7}$$

For j = 1,....,5

where q" is the source per unit area and equals $q_j \cdot L\Delta\bar{X}$.

For j = 6,

$$\theta_{j,i-1}^{n+1} - 2\left(1 + \frac{(L\Delta\bar{X}_j)^2}{\alpha_s \Delta t}\right)\theta_{j,i}^{n+1} + \theta_{j,i+1}^{n+1} = -\theta_{j,i-1}^{n} + 2\left(1 - \frac{(L\Delta\bar{X}_j)^2}{\alpha_s \Delta t}\right)\theta_{j,i}^{n} - \theta_{j,i+1}^{n} \tag{8a}$$

$\theta_j < \theta_f - \Delta\theta$

$$\theta_{j,i-1}^{n+1} - 2\left(1 + \frac{(L\Delta\bar{x}_j)^2}{\alpha_w \Delta t}\right)\theta_{j,i}^{n+1} + \theta_{j,i+1}^{n+1} = -\theta_{j,i-1}^{n}$$
$$+ 2\left(1 - \frac{(L\Delta\bar{x}_j)^2}{\alpha_w \Delta t}\right)\theta_{j,i}^{n} - \theta_{j,i+1}^{n} \qquad \theta_j > \theta_f + \Delta\theta \tag{8b}$$

$$k^- \theta_{j,i-1}^{n+1} - \left(k^+ + k^- + \frac{2C^*(L\Delta\bar{x}_j)^2}{\Delta t}\right)\theta_{j,i}^{n+1} + k^+\theta_{j,i+1}^{n+1} =$$
$$-k^-\theta_{j,i-1}^{n} + \left(k^+ + k^- - \frac{2C^*(L\Delta\bar{x}_j)^2}{\Delta t}\right)\theta_{j,i}^{n} - k^+\theta_{j,i+1}^{n}. \tag{8c}$$
$$\theta_f - \Delta\theta \le \theta_j \le \theta_f + \Delta\theta$$

where
$$k^+ = k_s + \frac{(k_w - k_s)}{2\Delta\theta}\left[\frac{\theta_{j,i+1}^{n+1/2} + \theta_{j,i}^{n+1/2}}{2} - (\theta_f - \Delta\theta)\right]$$
$$k^- = k_s + \frac{(k_w - k_s)}{2\Delta\theta}\left[\frac{\theta_{j,i-1}^{n+1/2} + \theta_{j,i}^{n+1/2}}{2} - (\theta_f - \Delta\theta)\right]$$
$$C^* = \frac{\lambda}{2T_{ref}\Delta\theta} + \frac{f_s C_s + C_w f_w}{2}$$

The value of the temperature at the half level in time is obtained from a truncated Taylor Series as follows:

$$\theta_{j,i}^{n+1/2} = \theta_{j,i}^{n} + \frac{\Delta t}{2}\left(\frac{\partial\theta_j}{\partial t}\right)_i^n + O(\Delta t)^2 \tag{8d}$$

The time derivative in the above analog is obtained from the equation (3') as

$$L^2 C^*\left(\frac{\partial\theta_j}{\partial t}\right)_i^n = k_1^+\left(\frac{\theta_{j,i+1}^{n} - \theta_{j,i}^{n}}{(\Delta\bar{x})^2}\right) - k_1^-\left(\frac{\theta_{j,i}^{n} - \theta_{j,i-1}^{n}}{(\Delta\bar{x})^2}\right) \tag{8e}$$

where

$$k_1^+ = k_s + \frac{k_w - k_s}{2\Delta\theta}\left[\frac{\theta^n_{j,i+1} + \theta^n_{j,i}}{2} - \left(\theta_f - \Delta\theta\right)\right]$$

$$k_1^- = k_s + \frac{k_w - k_s}{2\Delta\theta}\left[\frac{\theta^n_{j,i} + \theta^n_{j,i-1}}{2} - \left(\theta_f - \Delta\theta\right)\right]$$

$$C^* = \frac{\lambda}{2\,T_{ref}\,\Delta\theta} + \frac{\rho_s C_s + \rho_w C_w}{2}$$

Substituting (8e) into (8d) yields the finite-difference analog for $\theta^{n+\frac{1}{2}}_{j,1}$ as

$$\theta^{n+1/2}_{j,i} = \theta^n_{j,i} + \frac{\Delta t}{2C^*L^2}\left[k_1^+\left(\frac{\theta^n_{j,i+1} - \theta^n_{j,i}}{\Delta\bar{x}^2}\right) - k_1^-\left(\frac{\theta^n_{j,i} - \theta^n_{j,i-1}}{\Delta\bar{x}^2}\right)\right] \qquad (8f)$$

For $\theta^{n+\frac{1}{2}}_{j,i+1}$ and $\theta^{n+\frac{1}{2}}_{j,i-1}$ the finite-difference analogs are obtained in a similar manner and are given below.

$$\theta^{n+1/2}_{j,i+1} = \theta^n_{j,i+1} + \frac{\Delta t}{2C^*L^2}\left[k_2^+\left(\frac{\theta^n_{j,i+2} - \theta^n_{j,i+1}}{(\Delta\bar{x})^2}\right) - k_2^-\left(\frac{\theta^n_{j,i+1} - \theta^n_{j,i}}{(\Delta\bar{x})^2}\right)\right] \qquad (8g)$$

where

$$k_2^+ = k_s + \frac{k_w - k_s}{2\Delta\theta}\left[\frac{\theta^n_{j,i+2} + \theta^n_{j,i+1}}{2} - \left(\theta_f - \Delta\theta\right)\right]$$

$$k_2^- = k_s + \frac{k_w - k_s}{2\Delta\theta}\left[\frac{\theta^n_{j,i+1} + \theta^n_{j,i}}{2} - \left(\theta_f - \Delta\theta\right)\right]$$

$$C^* = \frac{\lambda}{2\,T_{ref}\,\Delta\theta} + \frac{\rho_s C_s + \rho_w C_w}{2}$$

$$\theta^{n+1/2}_{j,i-1} = \theta^n_{j,i-1} + \frac{\Delta t}{2C^*L^2}\left[k_3^+\left(\frac{\theta^n_{j,i} - \theta^n_{j,i-1}}{(\Delta\bar{x})^2}\right) - k_3^-\left(\frac{\theta^n_{j,i-1} - \theta^n_{j,i-2}}{(\Delta\bar{x})^2}\right)\right] \qquad (8h)$$

where $$k_3^+ = k_s + \frac{k_\omega - k_s}{2\Delta\theta}\left[\frac{\theta^n_{j,i} + \theta^n_{j,i-1}}{2} - \left(\theta_f - \Delta\theta\right)\right]$$

$$k_3^- = k_s + \frac{k_\omega - k_s}{2\Delta\theta}\left[\frac{\theta^n_{j,i-1} + \theta^n_{j,i-2}}{2} - \left(\theta_f - \Delta\theta\right)\right]$$

$$C^* = \frac{\lambda}{2T_{ref}\Delta\theta} + \frac{f_s C_s + f_\omega C_\omega}{2}$$

Equation (7) is valid for all grid points within each of the j^{th} layers except for the ice layer, within which equations(8a,b,c) are applicable. Equation (8c) was obtained using the finite difference formulation suggested by Von Rosenberg(12) and the temperatures at the half levels in time were calculated applying the method devised by Douglas(30).

The finite-difference equations for the interfacial points, for the two boundary conditions and for the heater are discussed below.

1. Finite-Difference Equations At Interfacial Points

Let i be the interfacial point between the slab layers j and j+1 as shown in Figure 4a. At this point, the temperature and the heat fluxes are equal and equation (4') is valid. Substitution of the finite-difference equation (6a) into equation (4') yields:

$$\theta^n_{j,i} = \theta^n_{j+1,i} \qquad (9a)$$

$$-\frac{k_j}{4\Delta\bar{x}_j}\left(\theta^{n+1}_{j,i+1}-\theta^{n+1}_{j,i-1}+\theta^{n}_{j,i+1}-\theta^{n}_{j,i-1}\right)=$$
$$-\frac{k_{j+1}}{4\Delta\bar{x}_{j+1}}\left(\theta^{n+1}_{j+1,i+1}-\theta^{n+1}_{j+1,i-1}+\theta^{n}_{j+1,i+1}-\theta^{n}_{j+1,i-1}\right) \qquad (9b)$$

Since the boundary extends only to the i^{th} grid point for the j^{th} slab, the temperatures $\theta^{n}_{j,i+1}$ and $\theta^{n+1}_{j,i+1}$ are fictitious. In the same manner, $\theta^{n}_{j+1,i-1}$ and $\theta^{n+1}_{j+1,i-1}$ are fictitious. At the point i, the governing equation (7) when applied for the layers j and j+1 yields:

$$\theta^{n+1}_{j,i-1}-2\left(1+\frac{(L\Delta\bar{x}_j)^2}{\alpha_j\Delta t}\right)\theta^{n+1}_{j,i}+\theta^{n+1}_{j,i+1}=-\theta^{n}_{j,i-1}$$
$$-\frac{2L(\Delta\bar{x}_j)}{T_{ref}k_j}q''_j+2\left(1-\frac{(L\Delta\bar{x}_j)^2}{\alpha_j\Delta t}\right)\theta^{n}_{j,i}-\theta^{n}_{j,i+1} \qquad (10a)$$

$$\theta^{n+1}_{j+1,i-1}-2\left(1+\frac{(L\Delta\bar{x}_{j+1})^2}{\alpha_{j+1}\Delta t}\right)\theta^{n+1}_{j+1,i}+\theta^{n+1}_{j+1,i+1}=-\theta^{n}_{j+1,i-1}$$
$$-\frac{2L(\Delta\bar{x}_{j+1})}{T_{ref}k_{j+1}}q''_{j+1}+2\left(1-\frac{(L\Delta\bar{x}_{j+1})^2}{\alpha_{j+1}\Delta t}\right)\theta^{n}_{j+1,i}-\theta^{n}_{j+1,i+1} \qquad (10b)$$

Eliminating the fictitious temperatures between equations (9b,10a,b) and using equation (9a) yields the following applicable finite-difference equation at the interfacial nodes:

$$\theta^{n+1}_{j,i-1} - \left[\left(1 + \frac{(L\Delta\bar{X}_j)^2}{\alpha_j \Delta t}\right) + \left(\frac{k_{j+1}\Delta\bar{X}_j}{k_j \Delta\bar{X}_{j+1}}\right)\left(1 + \frac{(L\Delta\bar{X}_{j+1})^2}{\alpha_{j+1}\Delta t}\right)\right]\theta^{n+1}_{j,i}$$
$$+ \left(\frac{k_{j+1}\Delta\bar{X}_j}{k_j \Delta\bar{X}_{j+1}}\right)\theta^{n+1}_{j+1,i+1} = -\theta^{n}_{j,i-1} +$$
$$\left[\left(1 - \frac{(L\Delta\bar{X}_j)^2}{\alpha_j \Delta t}\right) + \left(1 - \frac{(L\Delta\bar{X}_{j+1})^2}{\alpha_{j+1}\Delta t}\right)\left(\frac{k_{j+1}\Delta\bar{X}_j}{k_j \Delta\bar{X}_{j+1}}\right)\right]\theta^{n}_{j,i} \qquad (11)$$
$$- \left(\frac{k_{j+1}\Delta\bar{X}_j}{k_j \Delta\bar{X}_{j+1}}\right)\theta^{n}_{j+1,i+1} - \frac{L}{T_{ref}}\left[\frac{q''_j(\Delta\bar{X}_j)}{k_j} + \left(\frac{q''_{j+1}(\Delta\bar{X}_{j+1})}{k_{j+1}}\right)\left(\frac{k_{j+1}\Delta\bar{X}_j}{k_j \Delta\bar{X}_{j+1}}\right)\right]$$

The above equation (11) is applicable only if the governing equation (7) holds for the layers on either side of the interfacial node.

2. Finite-Difference Equation For The Ice-Abrasion Shield Interface

If i is the interfacial boundary point at the ice and abrasion shield interface, as shown in Figure 4b, it becomes necessary to consider which of the governing equations (8a,b,c) are applicable along with equation (7) for the abrasion shield and the boundary conditions (9a,b). Initially, the interface temperature is less than $\theta_f - \Delta\theta$ and, therefore, equation (8a) is used. For j = 5 at node i, equation (7) becomes (with $q''_5 = 0$),

$$\theta^{n+1}_{5,i-1} - 2\left(1 + \frac{(L\Delta\bar{X}_5)^2}{\alpha_5 \Delta t}\right)\theta^{n+1}_{5,i} + \theta^{n+1}_{5,i+1} =$$
$$-\theta^{n}_{5,i-1} + 2\left(1 - \frac{(L\Delta\bar{X})^2}{\alpha_5 \Delta t}\right)\theta^{n}_{5,i} - \theta^{n}_{5,i+1}. \qquad (12a)$$

For j = 6 at point i, equation (8a) reduces to

$$\theta^{n+1}_{6,i-1} - 2\left(1 + \frac{(L\Delta\bar{x}_6)^2}{\alpha_s \Delta t}\right)\theta^{n+1}_{6,i} + \theta^{n+1}_{6,i+1} = -\theta^{n}_{6,i-1} - \theta^{n}_{6,i+1} + 2\left(1 - \frac{(L\Delta\bar{x}_6)^2}{\alpha_s \Delta t}\right)\theta^{n}_{6,i} \tag{12b}$$

and the boundary conditions (9a,b) give:

$$\theta^{n}_{6,i} = \theta^{n}_{5,i} \tag{12c}$$

$$-\frac{k_s}{4\Delta\bar{x}_6}\left[\theta^{n+1}_{6,i+1} - \theta^{n+1}_{6,i-1} + \theta^{n}_{6,i+1} - \theta^{n}_{6,i-1}\right] = -\frac{k_5}{4\Delta\bar{x}_5}\left[\theta^{n+1}_{5,i+1} - \theta^{n+1}_{5,i-1} + \theta^{n}_{5,i+1} - \theta^{n}_{5,i-1}\right] \tag{12d}$$

The temperatures $\theta^{n}_{5,i+1}$, $\theta^{n+1}_{5,i+1}$, $\theta^{n}_{6,i-1}$ and $\theta^{n+1}_{6,i-1}$ are fictitious and have to be eliminated between the equations (12a,b,c,d) to give:

$$\theta^{n+1}_{5,i-1} - \left[\left(1 + \frac{(L\Delta\bar{x}_5)^2}{\alpha_5 \Delta t}\right) + \frac{k_s \Delta\bar{x}_5}{k_5 \Delta\bar{x}_6}\left(1 + \frac{(L\Delta\bar{x}_6)^2}{\alpha_6 \Delta t}\right)\right]\theta^{n+1}_{5,i} + \left(\frac{k_s \Delta\bar{x}_5}{k_5 \Delta\bar{x}_6}\right)\theta^{n+1}_{6,i+1} = -\theta^{n}_{5,i-1} - \left(\frac{k_s \Delta\bar{x}_5}{k_5 \Delta\bar{x}_6}\right)\theta^{n}_{6,i+1} + \left[\left(1 - \frac{(L\Delta\bar{x}_5)^2}{\alpha_5 \Delta t}\right) + \frac{k_s \Delta\bar{x}_5}{k_5 \Delta\bar{x}_6}\left(1 - \frac{(L\Delta\bar{x}_6)^2}{\alpha_6 \Delta t}\right)\right]\theta^{n}_{5,i} \tag{13a}$$

If the temperature at node i, $\theta^{n}_{6,i}$, is between $\theta_f - \Delta\theta$ and $\theta_f + \Delta\theta$, equation (8c) is used along with equation (12a,c,d)

and, as before, the fictitious temperatures $\theta^{n}_{5,i+1}$, $\theta^{n+1}_{5,i+1}$, $\theta^{n}_{6,i-1}$ and $\theta^{n+1}_{6,i-1}$ are eliminated to give:

$$\theta^{n+1}_{5,i-1} - \left[\left(1+\frac{(L\Delta\bar{X}_5)^2}{\alpha_5\Delta t}\right)+\frac{\Delta\bar{X}_5 k^*_i}{2\Delta\bar{X}_6 k_5 k^-}\left(k^+ + k^- + \frac{2C^*(L\Delta\bar{X}_6)^2}{\Delta t}\right)\right]\theta^{n+1}_{5,i}$$
$$+\frac{\Delta\bar{X}_5 k^*_i}{2\Delta\bar{X}_6 k_5 k^-}\left(k^+ + k^-\right)\theta^{n+1}_{6,i+1} = -\theta^{n}_{5,i-1}$$
$$+\left[\left(1-\frac{(L\Delta\bar{X}_5)^2}{\alpha_5\Delta t}\right)+\frac{\Delta\bar{X}_5 k^*_i}{2\Delta\bar{X}_6 k_5 k^-}\left(k^+ + k^- - \frac{2C^*(L\Delta\bar{X}_6)^2}{\Delta t}\right)\right]\theta^{n}_{5,i} \qquad (13b)$$
$$-\frac{\Delta\bar{X}_5 k^*_i}{2\Delta\bar{X}_6 k_5 k^-}\left(k^+ + k^-\right)\theta^{n}_{6,i+1}.$$

$$k^*_i = k_s + \frac{k_w - k_s}{2\Delta\theta}\left[\theta^{n+1/2}_{6,i} - \left(\theta_f - \Delta\theta\right)\right]$$

If the temperature at the interface i, $\theta^{n}_{6,i}$, is greater than $\theta_f+\Delta\theta$, equation (8b) is applied along with equations (12a,c,d). Again fictitious temperatures are eliminated to yield the applicable equation:

$$\theta^{n+1}_{5,i-1} - \left[\left(1+\frac{(L\Delta\bar{X}_5)^2}{\alpha_5\Delta t}\right)+\frac{k_w\Delta\bar{X}_5}{k_5\Delta\bar{X}_6}\left(1+\frac{(L\Delta\bar{X}_6)^2}{\alpha_w\Delta t}\right)\right]\theta^{n+1}_{5,i}$$
$$+\left(\frac{k_w\Delta\bar{X}_5}{k_5\Delta\bar{X}_6}\right)\theta^{n+1}_{6,i+1} = -\theta^{n}_{5,i-1} - \left(\frac{k_w\Delta\bar{X}_5}{k_5\Delta\bar{X}_6}\right)\theta^{n}_{6,i+1} \qquad (13c)$$
$$+\left[\left(1-\frac{(L\Delta\bar{X}_5)^2}{\alpha_5\Delta t}\right)+\frac{k_w\Delta\bar{X}_5}{k_5\Delta\bar{X}_6}\left(1-\frac{(L\Delta\bar{X}_6)^2}{\alpha_w\Delta t}\right)\right]\theta^{n}_{5,i}.$$

3. Finite-Difference Equation For The Substrate-Ambient Boundary

The interface under consideration is shown in Figure 4c. At this grid point i equals 1. The point i equals 0

is a fictitious point as it falls out of the composite body boundary. At i equals 1, the governing equation (7) is applicable along with the boundary condition (5a'). The finite-difference representation of equation (5a') using equation (6a) gives, for j = i = 1,

$$\frac{k_1}{4\Delta\bar{x}_1}\left(\theta_{1,2}^{n+1}+\theta_{1,2}^{n}-\theta_{1,0}^{n+1}-\theta_{1,0}^{n}\right)=h_1 L\left[\left(\frac{\theta_{1,1}^{n+1}+\theta_{1,1}^{n}}{2}\right)-\theta_0\right] \tag{14a}$$

Similarly, the governing equation (7) reduces to

$$\theta_{1,0}^{n+1}-2\left(1+\frac{(L\Delta\bar{x}_1)^2}{\alpha_1\Delta t}\right)\theta_{1,1}^{n+1}+\theta_{1,2}^{n+1}=-\theta_{1,0}^{n}+2\left(1-\frac{(L\Delta\bar{x}_1)^2}{\alpha_1\Delta t}\right)\theta_{1,1}^{n}-\theta_{1,2}^{n} \tag{14b}$$

Eliminating the fictitious temperatures $\theta_{1,0}^{n}$, and $\theta_{1,0}^{n+1}$ between equations (14a,b) yields:

$$\theta_{1,2}^{n+1}-\left[\left(1+\frac{(L\Delta\bar{x}_1)^2}{\alpha_1\Delta t}\right)+\frac{\Delta\bar{x}_1 h_1 L}{k_1}\right]\theta_{1,1}^{n+1}=-\theta_{1,2}^{n}+\left[\left(1-\frac{(L\Delta\bar{x}_1)^2}{\alpha_1\Delta t}\right)+\frac{\Delta\bar{x}_1 h_1 L}{k_1}\right]\theta_{1,1}^{n}-\frac{2\Delta\bar{x}_1 L h_1\theta_0}{k_1} \tag{15}$$

4. Finite-Difference Equation For The Ice-Ambient Boundary

The interfacial point, as shown in Figure 4d, is the grid point m. The point m+1 falls outside the composite body boundary and is therefore a fictitious point which has to be eliminated. The governing equation (8a) for j = 6

when applied to point m is of the form:

$$\theta^{n+1}_{6,M-1} - 2\left(1+\frac{L^2(\Delta\bar{X}_6)^2}{\alpha_s \Delta t}\right)\theta^{n+1}_{6,M} + \theta^{n+1}_{6,M+1} = -\theta^{n}_{6,M-1} + 2\left(1-\frac{L^2(\Delta\bar{X}_6)^2}{\alpha_s \Delta t}\right)\theta^{n}_{6,M} - \theta^{n}_{6,M+1} \tag{16a}$$

As before, the boundary condition (5b'), after using the finite-difference representation (6a), becomes:

$$-\frac{k_s}{4\Delta\bar{X}_6}\left[\theta^{n+1}_{6,M+1} - \theta^{n+1}_{6,M-1} + \theta^{n}_{6,M+1} - \theta^{n}_{6,M-1}\right] = h_2 L\left[\left(\frac{\theta^{n+1}_{6,M}+\theta^{n}_{6,M}}{2}\right) - \theta_\infty\right] \tag{16b}$$

Elimination of the fictitious temperatures $\theta^{n}_{6,m+1}$ and $\theta^{n+1}_{6,m+1}$ between equations (16a,b) gives the finite-difference equation for the point m as:

$$\theta^{n+1}_{6,M-1} - \left[\left(1+\frac{(L\Delta\bar{X}_6)^2}{\alpha_s\Delta t}\right) + \frac{h_2 L\Delta\bar{X}_6}{k_s}\right]\theta^{n+1}_{6,M} = -\theta^{n}_{6,M-1} + \left[\left(1-\frac{(L\Delta\bar{X}_6)^2}{\alpha_s\Delta t}\right) + \frac{h_2 L\Delta\bar{X}_6}{k_s}\right]\theta^{n}_{6,M} - \frac{2h_2 L\Delta\bar{X}_6\theta_\infty}{k_s} \tag{16c}$$

In deriving equation (16c), it has been assumed that at the upper boundary, point m, ice is present and the governing equation (8a) is applicable. However, if instead of ice a "mushy" phase exists at this boundary, the governing equation (8c) is applied at point m to yield:

$$k^+\theta^{n+1}_{6,M+1} - \left[k^+ + k^- + \frac{2L^2C^*(\Delta\bar{X}_6)^2}{\Delta t}\right]\theta^{n+1}_{6,M} + k^-\theta^{n+1}_{6,M-1} = -k^-\theta^{n}_{6,M-1} + \left[k^+ + k^- - \frac{2L^2C^*(\Delta\bar{X}_6)^2}{\Delta t}\right]\theta^{n}_{6,M} - k^+\theta^{n}_{6,M+1} \tag{17a}$$

Equation (5b') after rearranging and using equation (6a) gives:

$$-\frac{k^*}{4\Delta\bar{X}_6}\left[\theta^{n+1}_{6,M+1}-\theta^{n+1}_{6,M-1}+\theta^{n}_{6,M+1}-\theta^{n}_{6,M-1}\right] = h_2 L\left[\left(\frac{\theta^{n+1}_{6,M}+\theta^{n}_{6,M}}{2}\right)-\theta_\infty\right] \tag{17b}$$

Elimination of the fictitious temperatures $\theta^{n}_{6,m+1}$ and $\theta^{n+1}_{6,m+1}$ between equation (17a,b) gives the finite-difference equation for the point m as:

$$\begin{aligned}\left(k^+ + k^-\right)\theta^{n+1}_{6,M-1} - \left[\left(k^+ + k^- + \frac{2C^*(L\Delta\bar{X}_6)^2}{\Delta t}\right) + \frac{2h_2 L k^+ \Delta\bar{X}_6}{k^*}\right]\theta^{n+1}_{6,M} = \\ -\frac{4h_2 L k^+ \Delta\bar{X}_6\theta_\infty}{k^*} - k^+\theta^{n}_{6,M-1} - k^-\theta^{n}_{6,M-1} \\ + \left[\left(k^+ + k^- - \frac{2C^*(L\Delta\bar{X}_6)^2}{\Delta t}\right) + \frac{2h_2 L k^+\Delta\bar{X}_6}{k^*}\right]\theta^{n}_{6,M}.\end{aligned} \tag{17c}$$

Finally, instead of ice or a "mushy" phase, water is present at the upper boundary, the governing equation (8b) is applied at point m to give:

$$\begin{aligned}\theta^{n+1}_{6,M-1} - 2\left(1+\frac{L^2(\Delta\bar{X}_6)^2}{\alpha_\omega\Delta t}\right)\theta^{n+1}_{6,M} + \theta^{n+1}_{6,M+1} = -\theta^{n}_{6,M-1} \\ + 2\left(1-\frac{L^2(\Delta\bar{X}_6)^2}{\alpha_\omega\Delta t}\right)\theta^{n}_{6,M} - \theta^{n}_{6,M+1}.\end{aligned} \tag{18a}$$

Applying the boundary condition (5b') in its finite-difference form:

$$-\frac{k_\omega}{4\Delta\bar{X}_6}\left[\theta^{n+1}_{6,M+1}-\theta^{n+1}_{6,M-1}+\theta^{n}_{6,M+1}-\theta^{n}_{6,M-1}\right] = h_2 L\left[\left(\frac{\theta^{n+1}_{6,M}+\theta^{n}_{6,M}}{2}\right)-\theta_\infty\right] \qquad (18b)$$

and eliminating the fictitious temperatures $\theta^{n}_{6,m+1}$ and $\theta^{n+1}_{6,m+1}$ between equations (18a,b) gives the finite-difference equation for the point m as:

$$\theta^{n+1}_{6,M-1}-\left[\left(1+\frac{(L\Delta\bar{X}_6)^2}{\alpha_\omega\Delta t}\right)+\frac{h_2 L\Delta\bar{X}_6}{k_\omega}\right]\theta^{n+1}_{6,M} = -\theta^{n}_{6,M-1} + \left[\left(1-\frac{(L\Delta\bar{X}_6)^2}{\alpha_\omega\Delta t}\right)+\frac{h_2 L\Delta\bar{X}_6}{k_\omega}\right]\theta^{n}_{6,M} - \frac{2h_2 L\Delta\bar{X}_6\theta_\infty}{k_\omega} \qquad (18c)$$

5. Finite-Difference Equation For a Point Source Positioned At An Interface Between Two Layers

If the heater is not of finite thickness, but is instead a point source at node i between slabs j and j+1, the finite-difference equation is obtained by using the governing equation (7) at point i for both the j^{th} and $j+1^{th}$ slab along with the boundary conditions:

$$\theta_{j,i} = \theta_{j+1,i} \qquad \text{For all n} \qquad (19a)$$

$$-k_j\frac{\partial\theta_j}{\partial\bar{X}}+\frac{q''L}{T_{ref}} = -k_{j+1}\frac{\partial\theta_{j+1}}{\partial\bar{X}} \qquad \text{For all n} \qquad (19b)$$

The above equation in finite-difference form becomes:

$$-\frac{k_j}{4\Delta\bar{x}_j}\left[\theta^{n+1}_{j,i+1}+\theta^{n}_{j,i+1}-\theta^{n+1}_{j,i-1}-\theta^{n}_{j,i-1}\right]+\frac{q''L}{T_{ref}}= -\frac{k_{j+1}}{4\Delta\bar{x}_{j+1}}\left[\theta^{n+1}_{j+1,i+1}+\theta^{n}_{j+1,i+1}-\theta^{n+1}_{j+1,i-1}-\theta^{n}_{j+1,i-1}\right] \tag{19c}$$

Equation (7) for the j^{th} and $j+1^{th}$ layers, when applied at node i without the internal heat generation term gives:

$$\theta^{n+1}_{j,i+1}-2\left(1+\frac{L^2(\Delta\bar{x}_j)^2}{\alpha_j\Delta t}\right)\theta^{n+1}_{j,i}+\theta^{n+1}_{j,i-1}=-\theta^{n}_{j,i-1}+2\left(1-\frac{L^2(\Delta\bar{x}_j)^2}{\alpha_j\Delta t}\right)\theta^{n}_{j,i}-\theta^{n}_{j,i+1} \tag{19d}$$

$$\theta^{n+1}_{j+1,i+1}-2\left(1+\frac{L^2(\Delta\bar{x}_{j+1})^2}{\alpha_{j+1}\Delta t}\right)\theta^{n+1}_{j+1,i}+\theta^{n+1}_{j+1,i-1}=-\theta^{n}_{j+1,i+1}-\theta^{n}_{j+1,i-1}+2\left(1-\frac{L^2(\Delta\bar{x}_{j+1})^2}{\alpha_{j+1}\Delta t}\right)\theta^{n}_{j+1,i} \tag{19e}$$

The temperatures $\theta^{n}_{j,i+1}$, $\theta^{n+1}_{j,i+1}$, $\theta^{n}_{j+1,i-1}$ and $\theta^{n+1}_{j+1,i-1}$ are fictitious temperatures and are eliminated between the equations (19a,c,d,e), giving the finite-difference equation applicable for a point heat source as:

$$\theta^{n+1}_{j,i-1}-\left[\left(1+\frac{L^2(\Delta\bar{x}_j)^2}{\alpha_j\Delta t}\right)+\left(\frac{k_{j+1}\Delta\bar{x}_j}{k_j\Delta\bar{x}_{j+1}}\right)\left(1+\frac{L^2(\Delta\bar{x}_{j+1})^2}{\alpha_{j+1}\Delta t}\right)\right]\theta^{n+1}_{j,i}+\theta^{n+1}_{j+1,i+1}\left(\frac{k_{j+1}\Delta\bar{x}_j}{k_j\Delta\bar{x}_{j+1}}\right)=-\theta^{n}_{j,i-1}-\left(\frac{k_{j+1}\Delta\bar{x}_j}{k_j\Delta\bar{x}_{j+1}}\right)\theta^{n}_{j+1,i+1}+\left[\left(1-\frac{L^2(\Delta\bar{x}_j)^2}{\alpha_j\Delta t}\right)+\left(\frac{k_{j+1}\Delta\bar{x}_j}{k_j\Delta\bar{x}_{j+1}}\right)\left(1-\frac{L^2(\Delta\bar{x}_{j+1})^2}{\alpha_{j+1}\Delta t}\right)\right]\theta^{n}_{j,i}-\frac{2q''L\Delta\bar{x}_j}{T_{ref}k_j} \tag{20}$$

IV. METHOD OF SOLUTION AND PROGRAM ALGORITHM

A. METHOD OF SOLUTION

The numerical formulation of the de-icer pad using the finite difference scheme results in a set of linear equations which can be put in tridiagonal matrix form. The equations are shown below and are readily solved using the Gaussian Elimination method suggested in Reference (31).

$$
\begin{aligned}
b_1\theta_1 + c_1\theta_2 &= d_1 \\
a_2\theta_1 + b_2\theta_2 + c_2\theta_3 &= d_2 \\
a_3\theta_2 + b_3\theta_3 + c_3\theta_4 &= d_3 \\
\cdots\cdots\cdots\cdots\cdots\cdots & \\
a_i\theta_{i-1} + b_i\theta_i + c_i\theta_{i+1} &= d_i \\
\cdots\cdots\cdots\cdots\cdots\cdots & \\
a_N\theta_{N-1} + b_N\theta_N &= d_N
\end{aligned}
\qquad (21)
$$

The complete algorithm for the solution of the tridiagonal system is

$$
\begin{aligned}
\theta_N &= G_N \\
\theta_i &= G_i - (c_i\theta_{i+1})/BE_i \,, \quad i = N-1, N-2, \ldots, 1
\end{aligned}
$$

$$
\text{where } BE_1 = b_1 \text{ and } G_1 = d_1/BE_1 \qquad (22)
$$

$$
\begin{aligned}
BE_i &= b_i - (a_i c_{i-1})/BE_{i-1}, \quad i = 2,3,\ldots,N \\
G_i &= (d_i - a_i G_{i-1})/BE_i, \quad i = 2,3,\ldots,N
\end{aligned}
$$

In the present study, non-dimensional temperatures, θ_i, at the time step, n+1, are calculated using the above algorithm. The constants d_1, d_2,.....,d_N are initially calculated using the temperatures, θ_i, at the previous time step, n.

B. NUMERICAL PROGRAM ALGORITHM

The flow diagram of the main program for the de-icer pad is shown in Figure 5. The computer program is listed in Appendix I.

V. NUMERICAL RESULTS

In order to test the resulting program and algorithm, an unsteady state heat conduction problem involving a two layered gypsum board-steel composite body was solved applying the procedure mentioned earlier in Chapters III and IV. The results are shown in Figure 6 and are in excellent agreement with the analytical solution given in Reference (31). The above problem applied convective boundary conditions at both boundaries; however, the computer model in this study has been designed to also handle constant temperature or mixed boundary conditions.

Initially, the de-icer pad problem was solved assuming no phase change in the ice layer and uniform heat input for both the point heat source and the finite thickness heaters. For the de-icer pad configuration shown in Figure 7, the temperature rise at the ice-abrasion shield interface in order to raise the interface temperature to 0° C is compared with the results obtained numerically by Stallabrass (4) and analytically by Campbell (3). As shown in Figure 7, excellent agreement is achieved between the two numerical methods and the analytical solution, up to 5 seconds. Beyond 5 seconds, the numerical solution of Stallabrass (4) gives a slightly optimistic temperature rise, while the present

method shows continued excellent agreement with the analytical solution.

To determine the effect of the various variables on the de-icing time, a number of cases were investigated and, whenever possible, compared with the results of Stallabrass (4). In Figure 7, as well as in all of the following cases, values of h_1 = 1 Btu/ft^{2}hr°F and h_2 = ∞ were used.

A. EFFECT OF POWER DENSITY

The de-icing time in the present study is assumed to be the time interval beginning when power is applied to the heater and extending up until the ice-abrasion shield interface just reaches a temperature of 32 °F. Figure 8 shows the results of the effect of variation in the power density on the de-icing time for various ambient temperatures. Good agreement is obtained with the results of Stallabrass (4). The slight variation occurs because of the more optimistic nature of Stallabrass' results as indicated in Figure 7. Figure 8 does demonstrate what actual tests have indicated, namely that the total energy required in order to shed the ice increases with a decrease in ambient temperature and with a decrease in the power density. Hence, lower power densities on the order of 15 or 20 watts/in^2 should not be used for low ambient conditions because of the long de-icing times that are needed. Tests have indicated that a power density on the order of 25 watts/in^2 is the practical minimum.

B. EFFECT OF INSULATION THICKNESS RATIO AND INSULATION MATERIAL

An insulation thickness of 0.010 inches has been assumed for the outer epoxy/glass insulation for the present study. Since it is desired that a maximum amount of energy released from the heater be directed toward the ice layer, the outer insulation should be thinner than the inner insulation. Figure 9 shows the effect of varying the insulation thickness ratio, inner insulation thickness/outer insulation thickness, on the de-icing time. As the ratio is increased from 1 through 5, the de-icing time decreases appreciably. For an ambient temperature of -25 °C, a reduction of 20% in the de-icing time occurs as the ratio is increased from 2 to 5. However, further increasing of the insulation thickness ratio only affects the de-icing time for lower ambient conditions. As shown in Figure 9 for an ambient temperature of -25 °C, the de-icing time does not change for an increase in thickness ratio from 5 to 10, although it does for lower ambient temperatures.

A decrease in the de-icing time may also be achieved by changing the inner insulation material. Figure 10 shows the effect on the de-icing time when the epoxy/glass insulation of 0.22 Btu/hr ft °F thermal conductivity is replaced by the same thickness of polytetrafluoroethylene (KEL-F) having 0.04 Btu/hr ft °F thermal conductivity. For an ambient temperature of -25 °C, the de-icing time is reduced by

approximately 36%. Hence it is advantageous to use an insulation material of very low thermal conductivity if it is also a good electrical insulator.

C. EFFECT OF SUBSTRATE MATERIAL

Figure 11 shows the effect on the de-icing time for various types of substrate materials. It might be expected that if the aluminum alloy is replaced by stainless steel, which has a lower thermal conductivity and thermal diffusivity, the de-icing time would be reduced; however, just the opposite occurs. This result is attributed to the higher thermal capacity per unit volume of the stainless steel. Figure 11 also shows that if an insulation layer of 0.087 inch epoxy/glass is added to the aluminum alloy substrate, thereby reducing the overall thermal conductivity of the substrate, a decrease in the de-icing time is observed.

D. EFFECT OF VARIABLE HEAT INPUT

In the previous sections, the heat input was assumed uniform and constant. In this section, a step-wise heat input is applied and the temperature response at all the interfacial nodes is determined. Figures 12 a and b show the temperature response for a variable point heat source (3 seconds on, 1 second off) as compared to a constant point heat source for an ambient temperature of 5 °F (-15 °C). As expected, the temperatures at the various interfacial nodes drop as the heat is switched off, and begin to rise

again as the heat is switched on. Figures 13 a and b show the corresponding results for a 5 seconds on, 1 second off, finite thickness heater for an ambient temperature of -22 °F (-30 °C). Thus, if heat is applied such that the heater is on for a period until the ice-abrasion shield interface reaches a temperature of 32 °F, and then is switched off until another layer of ice forms on the blade surface, the total energy usage for de-icing would be reduced. The computer program in this study has used an arbitrary periodic step-wise heat input, but it can be modified to apply to any other type of variable heat input.

E. EFFECT OF PHASE CHANGE

In the earlier part of this study, as in the work of Stallabrass (4), the phase change in the ice layer has been neglected. Hence, optimistic de-icing times were obtained because the latent heat needed to melt the ice has been ignored. To rectify this, a method used by Bonacina et al. (26) is applied to account for the phase change in the ice layer. In order to test the accuracy of this method, the one-dimensional water-ice solidification problem was solved.

As mentioned in Chapter II, the selection of the phase change temperature interval, $2\Delta T$, depends upon the physical problem and, in combination with the number of nodes in the ice layer, affects the accuracy of the solution. Figure 14 shows that a phase change temperature interval of 2 °F

provides good agreement with the results of Bonacina et al. (26). Figure 14 also indicates that increasing the number of nodes from 81 to 126 for the temperature interval of 2 °F does not affect the results. For the ice layer in the de-icer pad problem, various numbers of nodes were used to determine what effect, if any, they would have on the accuracy of the solution. It was observed that increasing the number of nodes above 60 did not change the solution and, therefore, for each of the solutions, 60 nodes were used in the ice layer.

As in the earlier sections, the de-icing time is assumed to be the time at which the interfacial temperature at the ice-abrasion shield interface reaches 32 °F. Figure 15 a is a repetition of Figure 7, but with the phase change being considered, and shows that the de-icing time is increased. This is expected since the latent heat of the ice is now accounted for, whereas in the previous cases the ice had been treated as a single phase. Figure 15 b parallels Figure 9 and Figure 15 c parallels Figure 11 in illustrating the same increasing time result. Thus, the results shown in Figures 15 a, b and c should therefore be more realistic.

VI. CONCLUSIONS AND RECOMMENDATIONS

The one-dimensional computer simulation model developed in this study for the de-icer pad configuration accurately predicts the temperature profiles for any type of boundary conditions or thermal heat sources. The results agree well with previous numerical calculations done by Stallabrass (4) for cases when the phase change is not considered. The method of Bonacina et al. (26) to describe the phase change was incorporated into the model and adequately predicts the thermal history of the de-icer pad when the latent heat effect of the ice is taken into account.

The next study should concentrate on developing a two-dimensional de-icer pad model in order to investigate the effects of blade shape, heater gap-width and heater geometry on the de-icing time.

REFERENCES

1. Werner, J. B., "Ice protection investigation for advanced rotary wing aircraft," Lockheed-California Report IR 25327-10, 1973.

2. Wardlaw, R. L., "An approximate method for estimating the transient heat flow distribution in a de-icing pad," NRC Lab Report LR-95, 1954.

3. Campbell, W. F., "A rapid analytical method for calculating the early transient temperature in a composite slab," NRC Lab Report MT-32, 1956.

4. Stallabrass, J. R., "Thermal aspects of de-icer design," presented at The International Helicopter Icing Conference, Ottawa, Canada, 1972.

5. Carslaw, H. S. and J. C. Jaeger, "Conduction of heat in solids," Clarendon Press, Oxford, 1959.

6. Goodman, T. R., "The adjoint heat conduction problem for solids," ASTIA-AD 254-769, (AFOSR-520), 1961.

7. Bouchillon, C. W., "Unsteady heat conduction in composite slabs," ASME Paper 64-WA/HT-13, 1964.

8. Tittle, C. W., "Boundary value problems in composite media: quasi-orthogonal functions," J. Appl. Phys. 36, 1486, 1965.

9. Tittle, C. W. and V. L. Robinson, "Analytical solution of conduction problems in composite media," ASME Paper 65-WA/HT-52, 1965.

10. Bulavin, P. E. and V. M. Kashcheev, "Solution of nonhomogenous heat conduction equation for multilayered bodies," Int. Chem. Engg. 5, 112, 1965.

11. Nogotov, E. F., "Applications of numerical heat transfer," McGraw-Hill, New York, 1978.

12. Von Rosenberg, D. V., "Methods for the numerical solution of partial differential equations," American Elsevier, New York, 1969.

13. Price, P. H. and M. R. Slack, "Stability and accuracy of numerical solutions of the heat flow equations," Brit. J. App. Phys. 3, 379, 1952.

14. Dusinberre, G. M., "A note on the implicit method for finite difference heat transfer calculations," J. Heat Trans. 92, 94, 1961.

15. Goodman, T. R., "The heat balance integral and its application to problems involving a change of phase," Trans. ASME 80, 335, 1958.

16. Citron, S. J., "Heat conduction in a melting slab," J. Aerosp. Sci. 27, 477, 1956.

17. Westphal, K. O., "Series solution of freezing problems with the fixed surface radiating into a medium of arbitrary varying temperature," Int. J. Heat-Mass Trans. 10, 195, 1967.

18. Mori, A. and K. Araki, "Methods for analysis of the moving boundary surface problem," Int. Chem. Engg. 16, 734, 1976.

19. Muehlbauer, J. C. and J. E. Sunderland, "Heat conduction with freezing or melting," App. Mech. Rev. 18, 951, 1965.

20. Rubinstein, K. I., "The Stefan problem," Trans. of Math. Monog., No. 27, American Mathematical Society, 1972.

21. Mastanaiah, K., "On the numerical solution of phase change problems in transient nonlinear heat conduction," Int. J. Num. Meth. in Engg. 10, 833, 1976.

22. Lazaridis, A., "A numerical solution of the multidimensional solidification problem," Int. J. Heat-Mass Trans. 13, 1459, 1970.

23. Crank, J., "Two methods for the numerical solution of moving boundary problems in diffusion and heat flow," Quart. J. of Mech. and App. Math. 10, 220, 1957.

24. Atthey, D. R., "A finite difference scheme for melting problems," J. Inst. Math. App. 13, 353, 1974.

25. Goodrich, L. E., "Efficient numerical technique for one-dimensional thermal problems with phase change," Int. J. Heat-Mass Trans. 21, 615, 1978.

26. Bonacina, C., Comini, G., Fasano, A. and N. Primicerio, "Numerical solution of phase change problems," Int. J. Heat-Mass Trans. 16, 1825, 1973.

27. Meyers, G. H., "Multidimensional Stefan problems," SIAM J. Num. Anal. 10, 522, 1973.

28. Shamsunder, N. and E. M. Sparrow, "Analysis of multi-dimensional conduction phase change via the enthalpy model," J. Heat Trans. 75, 333, 1975.

29. Comini, G., Delguidice, S., Lewis, R. W. and O. L. Zienkiewicz, "Finite element solution of nonlinear heat conduction problems with special reference to phase change," Int. J. Num. Meth. in Engg. 8, 613, 1974.

30. Douglas, J., "The application of stability analysis in the numerical solution of quasi-linear parabolic differential equations," Trans. Amer. Math. Soc. 89, 484, 1958.

31. Sugiyama, S., Nishimura, M., and S. Waianabe, "Transient temperature response to composite slab," Int. J. Heat-Mass Trans. 18, 875, 1974.

TABLE 1

THERMAL PROPERTIES OF SELECTED MATERIALS

Material	Thermal Conductivity $\frac{Btu}{hr.ft.°F}$	Thermal Conductivity $\frac{Cal}{sec.cm.°C}$	Spec. Heat Btu/lb.°F Cal/g°C	Diffusivity $\frac{ft^2}{hr.}$	Diffusivity $\frac{cm^2}{sec.}$	Density $\frac{lb.}{ft^3}$	Density $\frac{g}{cm^3}$
Aluminum (soft)	124	0.51	0.23	3.20	0.820	169	2.71
Aluminum Alloy, 75ST6	66.5	0.275	0.23	1.65	0.427	175	2.80
Nichrome 80/20	7.6	0.031	0.107	0.138	0.035	515	8.25
Stainless Steel 304	8.7	0.036	0.118	0.150	0.0385	495	7.93
Epoxy/Glass filled 32%	0.22	9×10^{-4}	0.23	0.0087	2.2×10^{-3}	110	1.82
Polytrifluoro-chloroethylene (KEL-F)	0.04	1.7×10^{-4}	0.216	0.0014	0.38×10^{-3}	130	2.08
Water (0°C)	0.320	1.32×10^{-3}	0.997	0.0051	0.00132	62.4	1.0
Ice (pure) 0°C	1.293	5.35×10^{-3}	0.5057	0.0445	0.0115	57.2	0.9168
-10°C	1.356	5.61×10^{-3}	0.5038	0.0469	0.0121	57.3	0.9182
-20°C	1.416	5.86×10^{-3}	0.5020	0.0492	0.0127	57.4	0.9196

Latent Heat of Fusion of Ice = 143.4 Btu/lb. = 79.75 Cal/g.

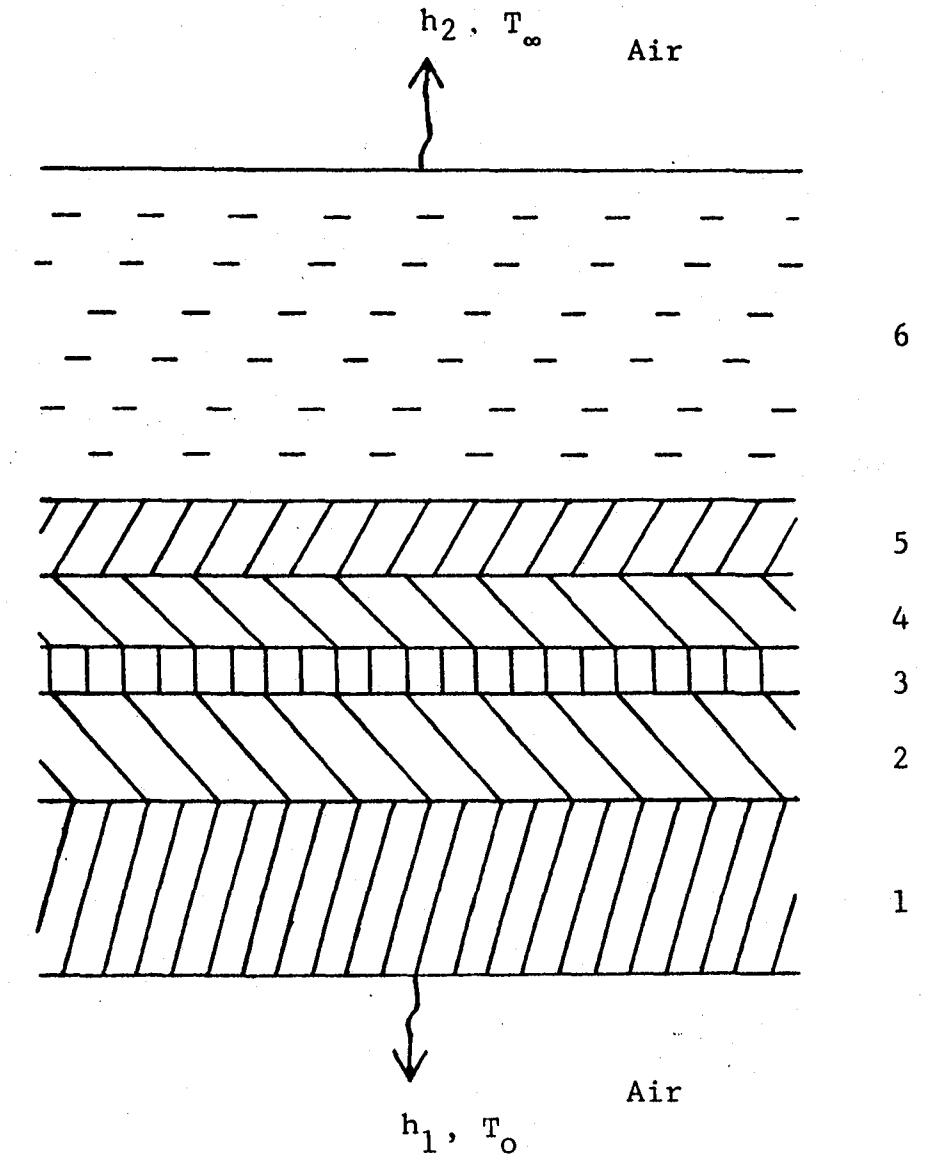

Figure 1. One Dimensional De-icing Pad Model

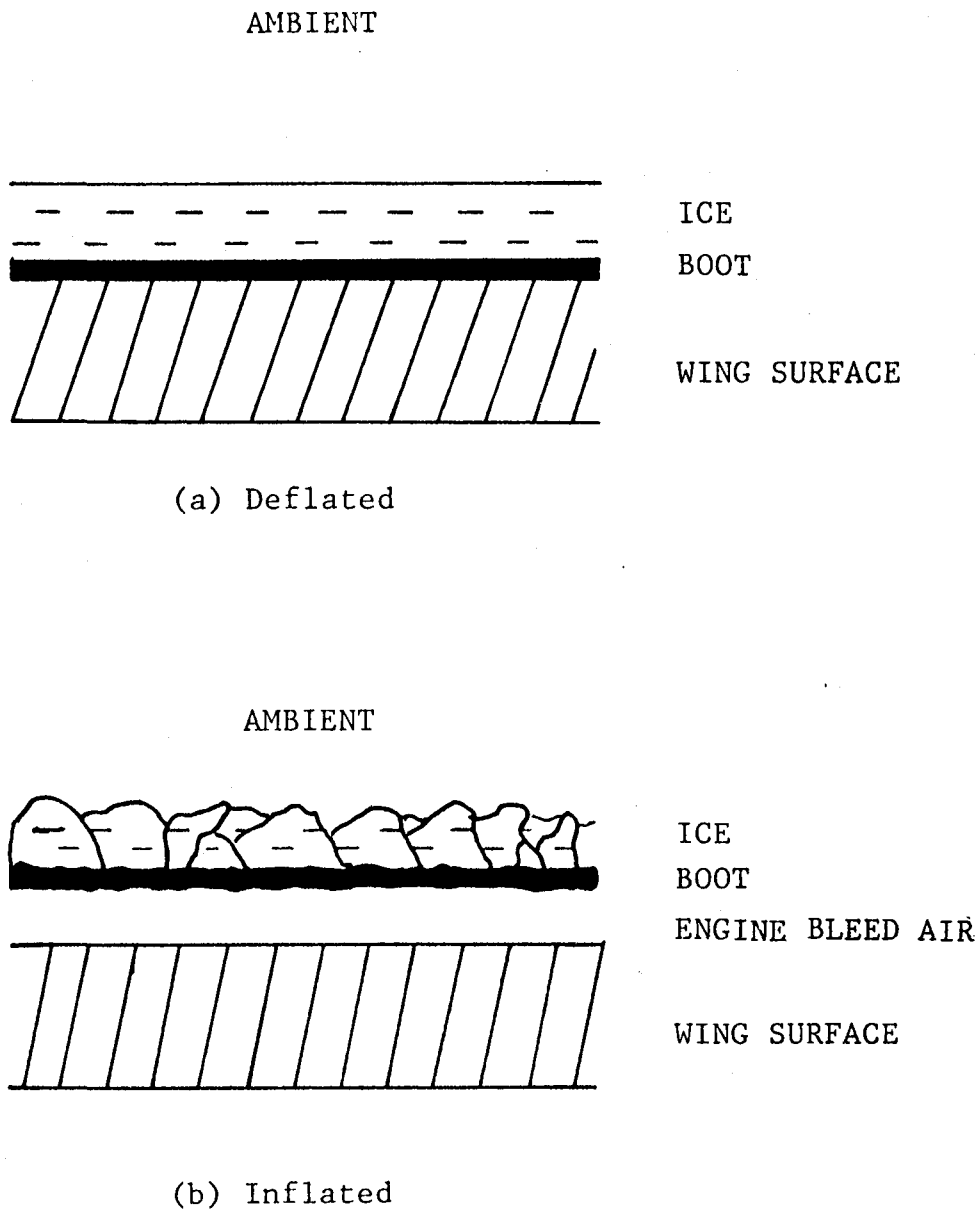

Figure 2. Section Of Wing Fitted With Pneumatic Boot

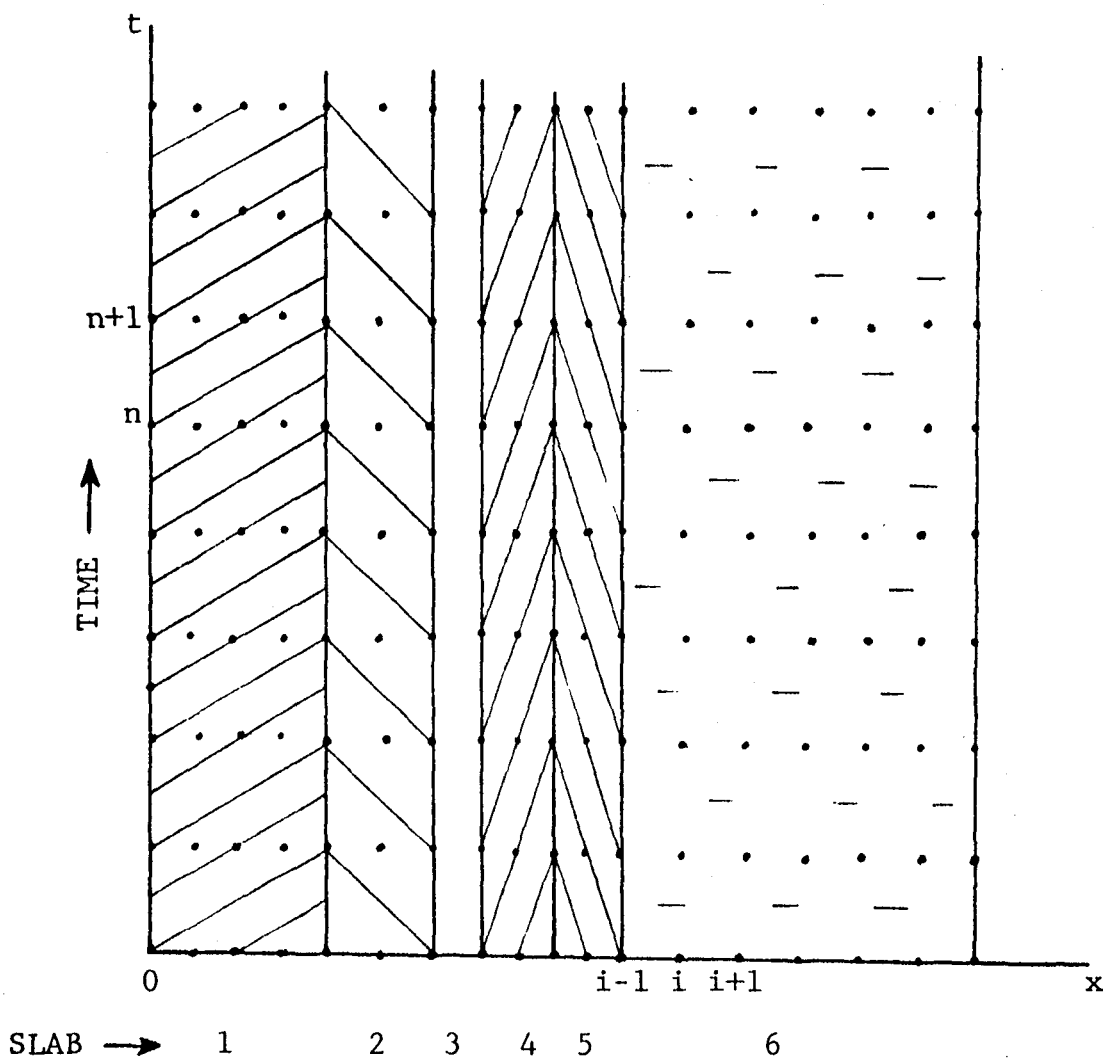

Figure 3. One Dimensional Finite-Difference De-icer Pad Model

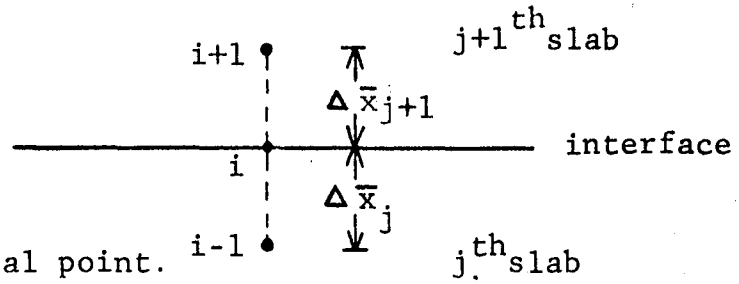

(a) Interfacial point.

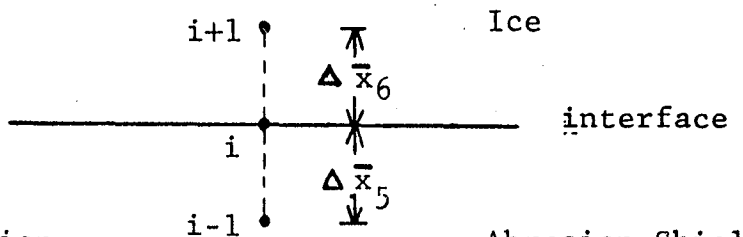

(b) Ice-Abrasion Shield Interface.

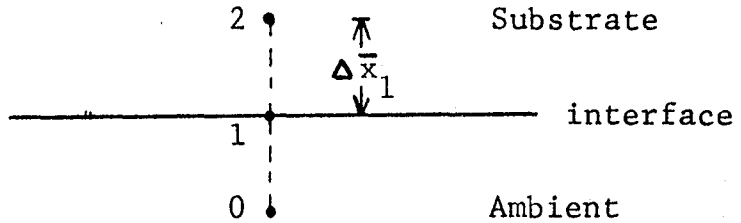

(c) Substrate-Ambient Interface.

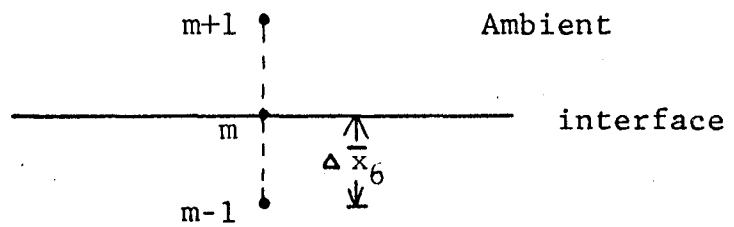

(d) Ice-Ambient Interface.

Figure 4. Finite Difference At Selected Grid Points

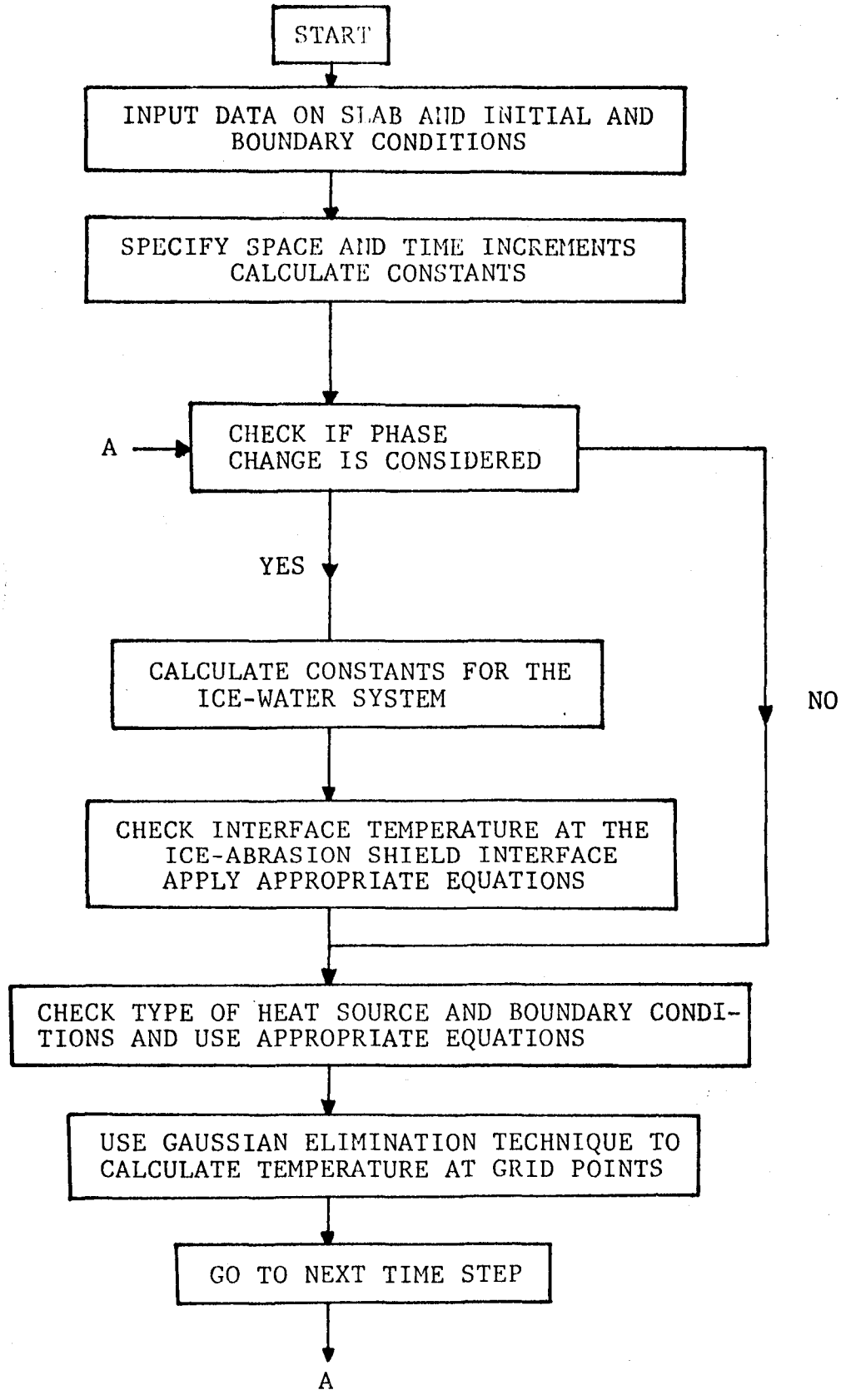

Figure 5. Flow Diagram Of Main Program

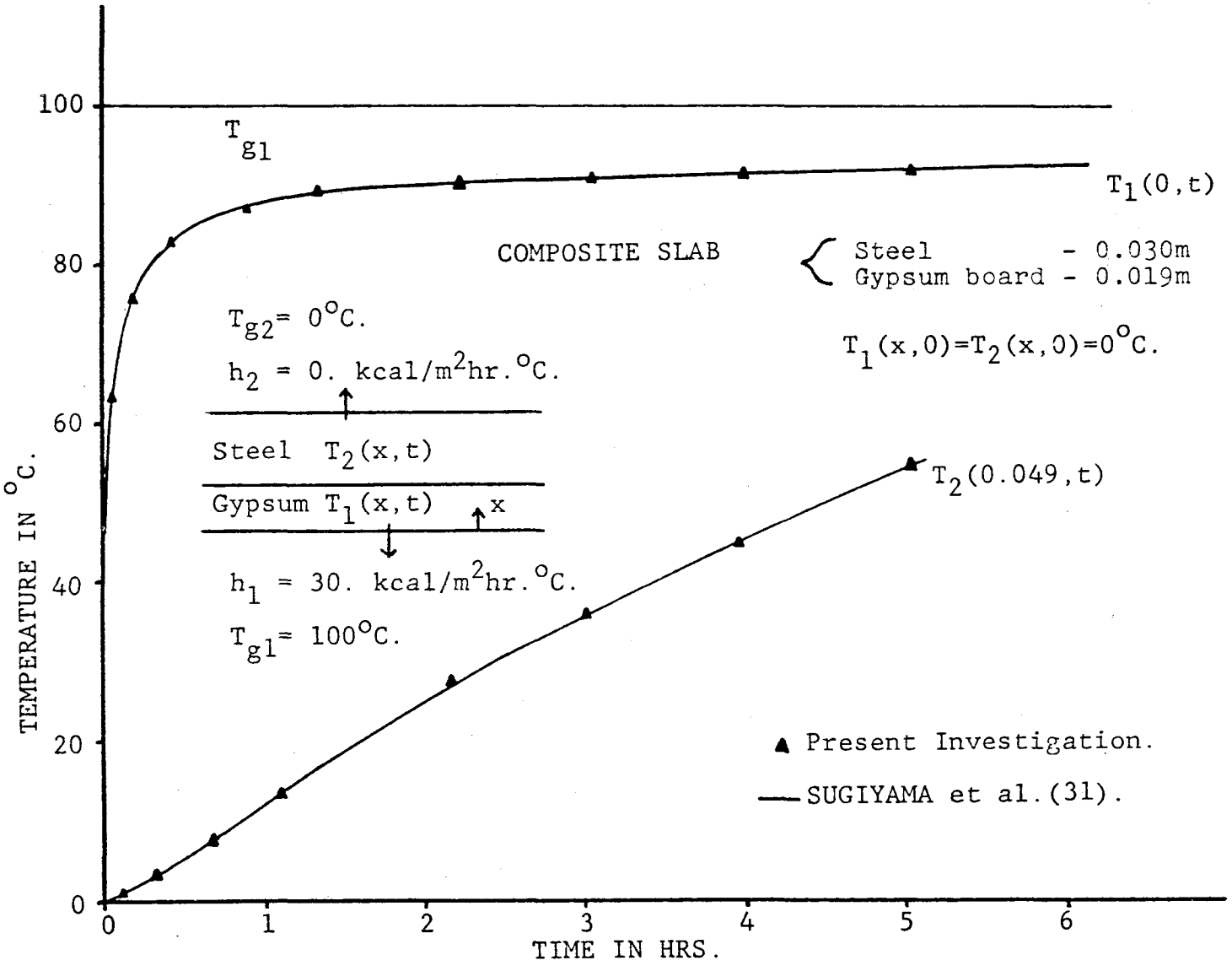

Figure 6. Comparsion Of Finite-Difference And Analytical Results For Composite Slab

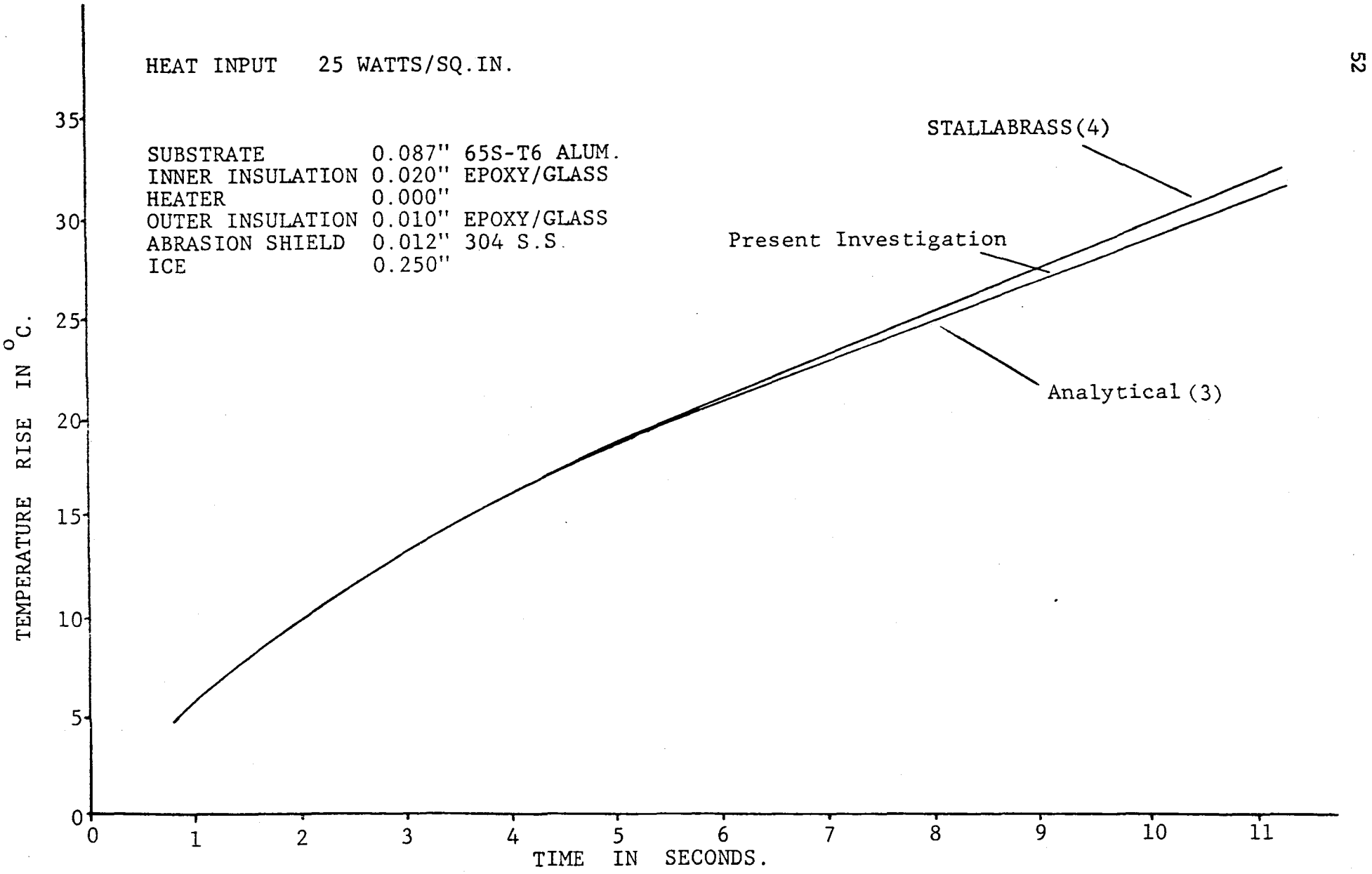

Figure 7. Comparison Of Finite-Difference And Analytical Results For De-icer Pad

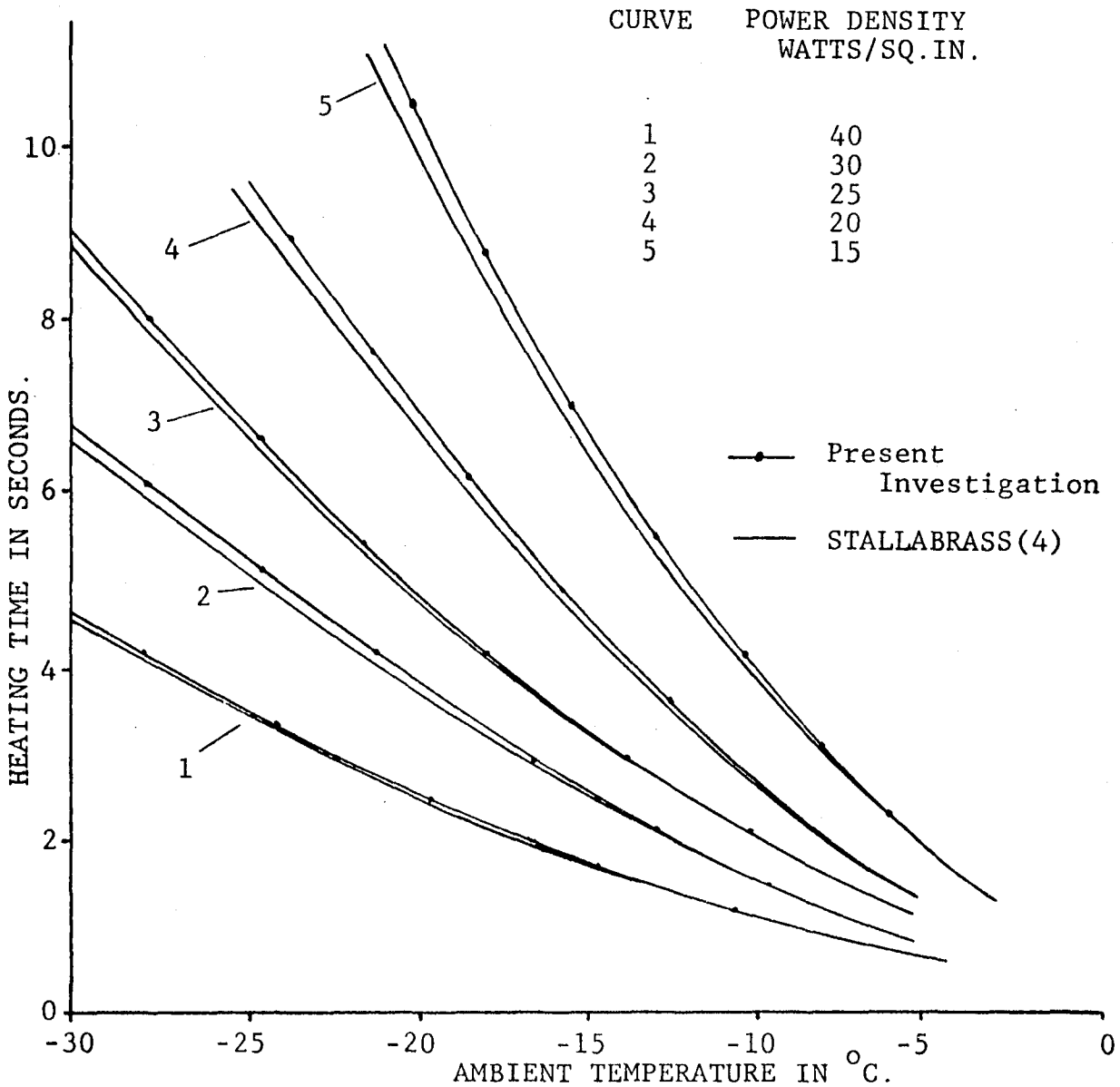

DE-ICER PAD CONSTRUCTION	SUBSTRATE	0.087" 75S-T6 ALUM.
	INNER INSULATION	0.050" EPOXY/GLASS
	HEATER	0.004" NICHROME
	OUTER INSULATION	0.010" EPOXY/GLASS
	ABRASION SHIELD	0.012" 304 S.S.
	ICE	0.250"

Figure 8. Effect Of Power Density On De-icer Performance

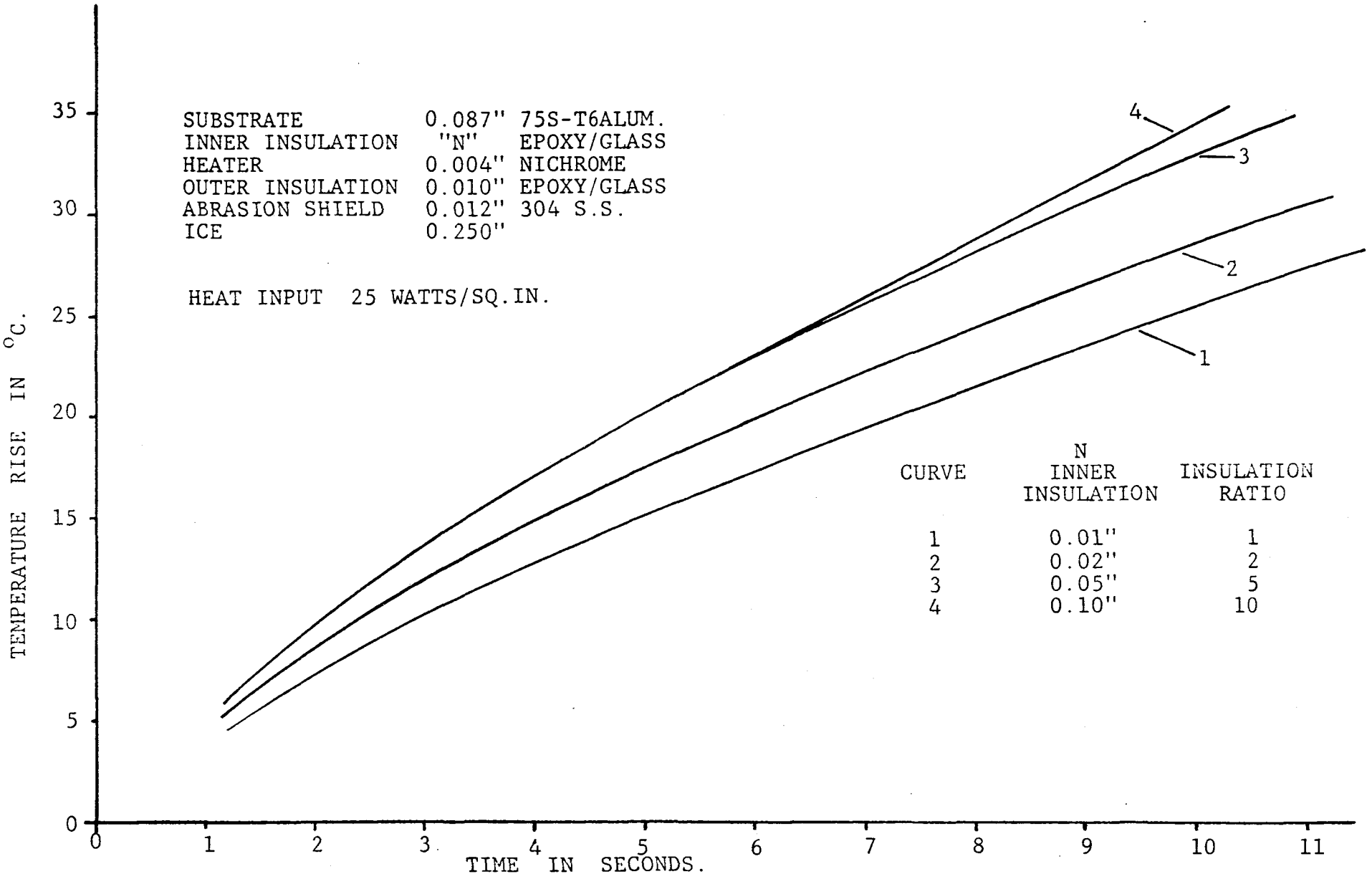

Figure 9. Comparison Of De-icing Time For Various Ratios Of Inner To Outer Insulation Thickness

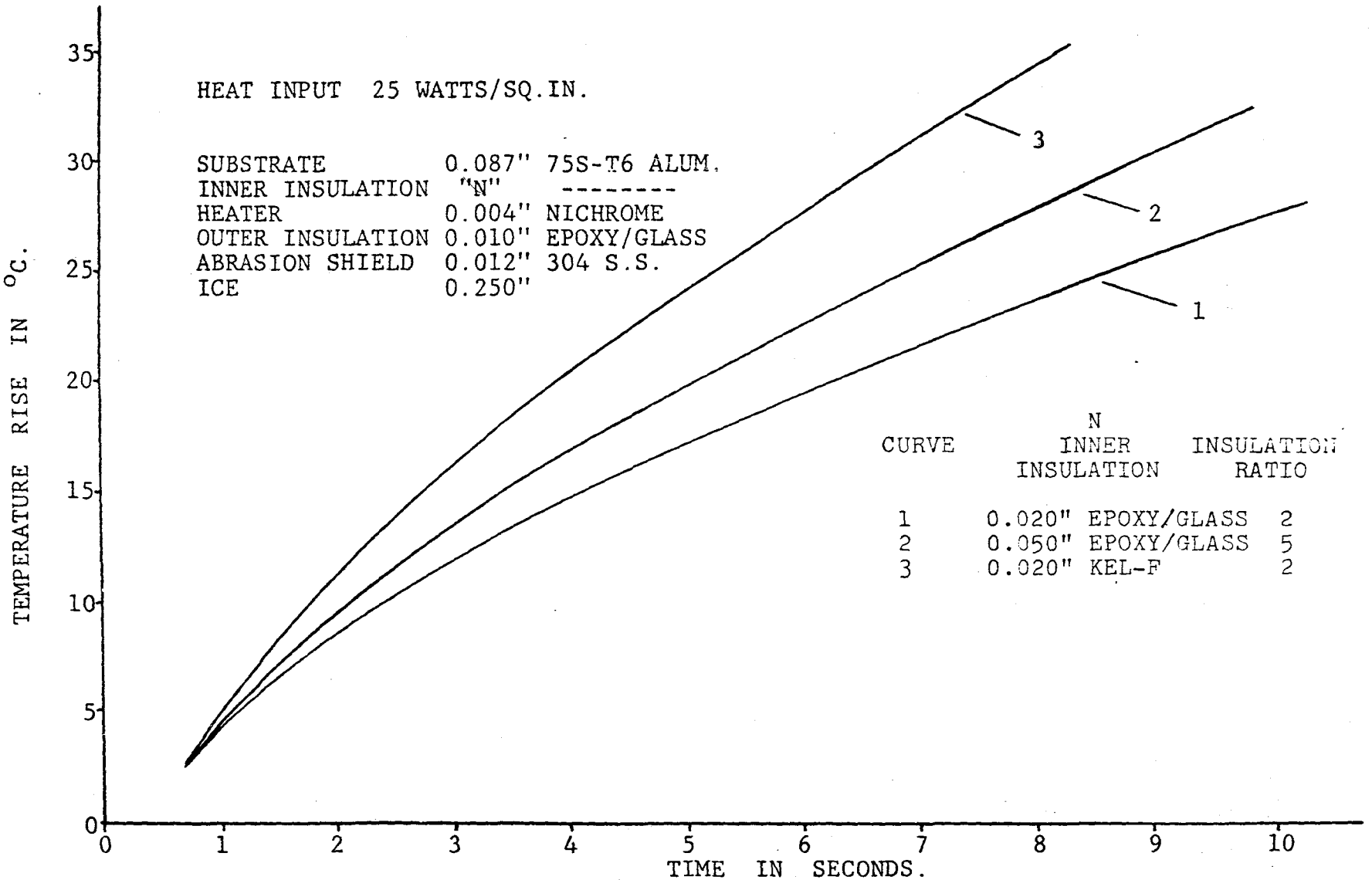

Figure 10. Effect Of Insulation Thickness Ratio And Material On De-icing Time

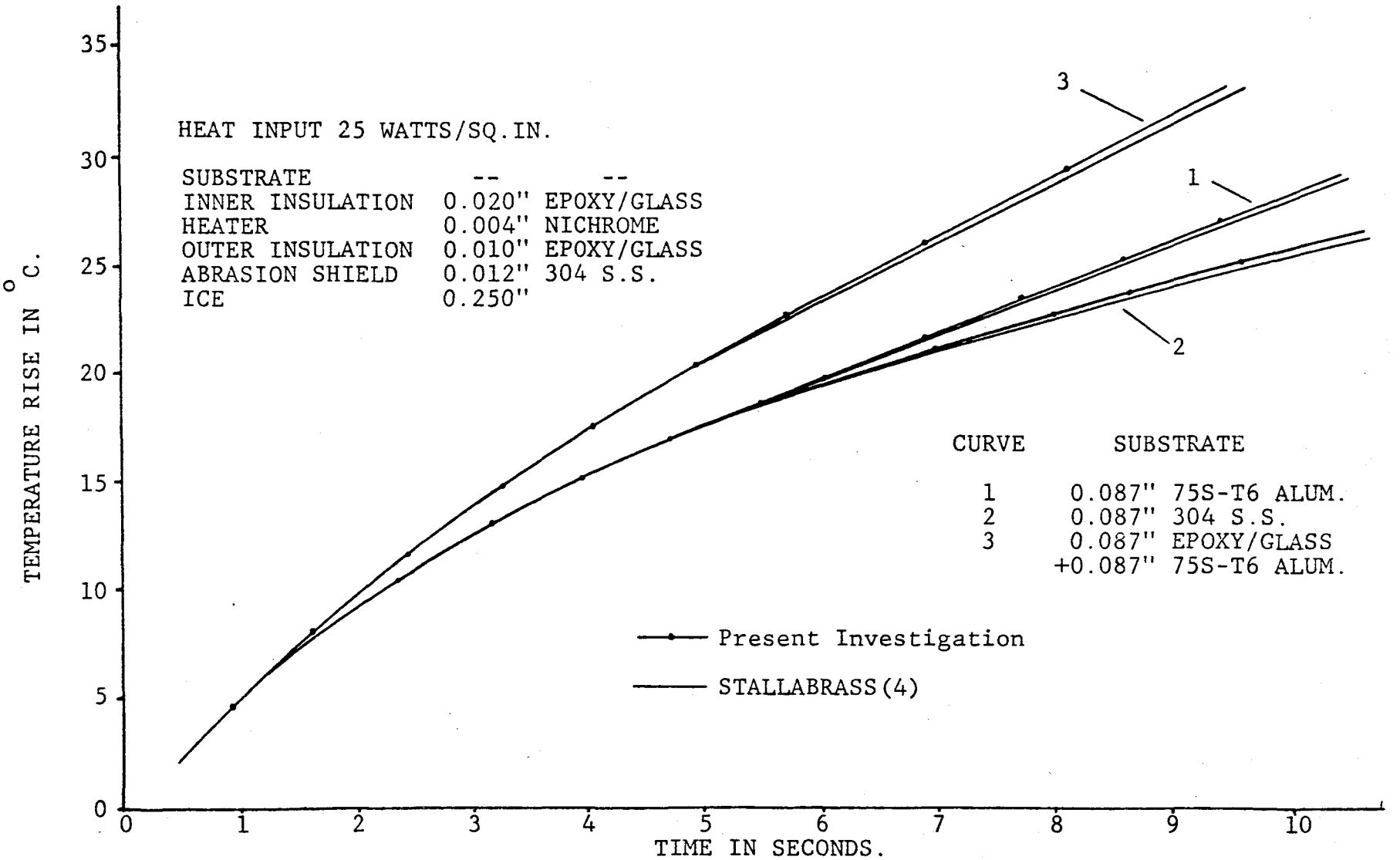

Figure 11. Comparison Of De-icing Time For Various Substrate Materials

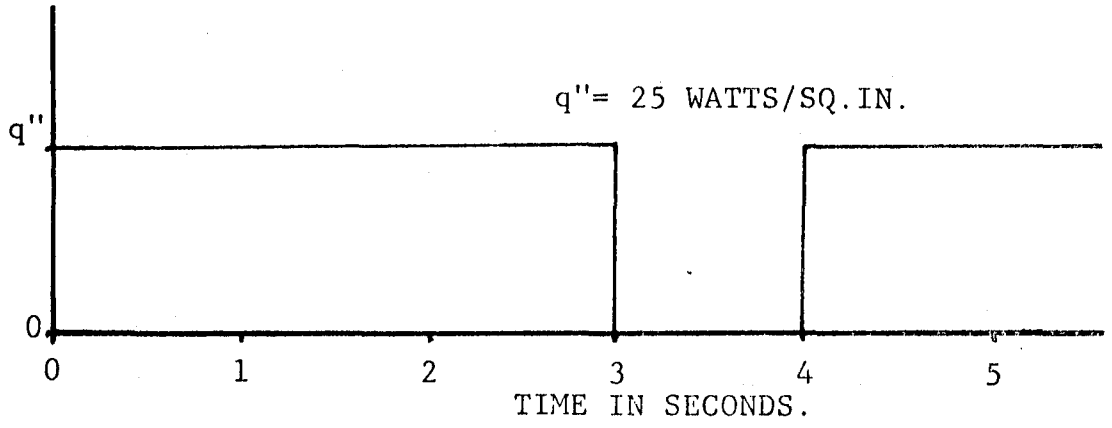

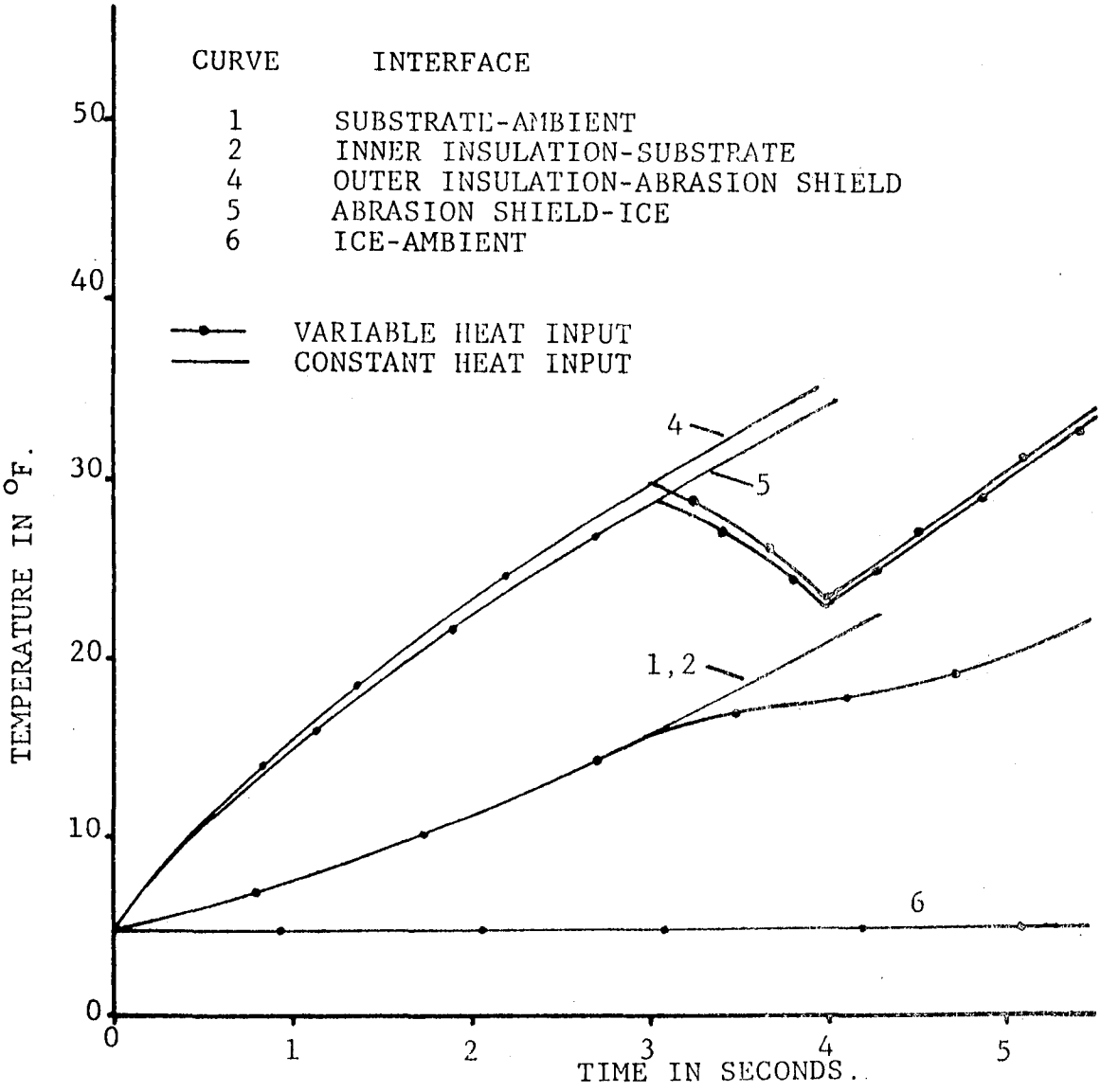

Figure 12a. Interfacial Temperature Response To Constant And Variable Point Heat Source

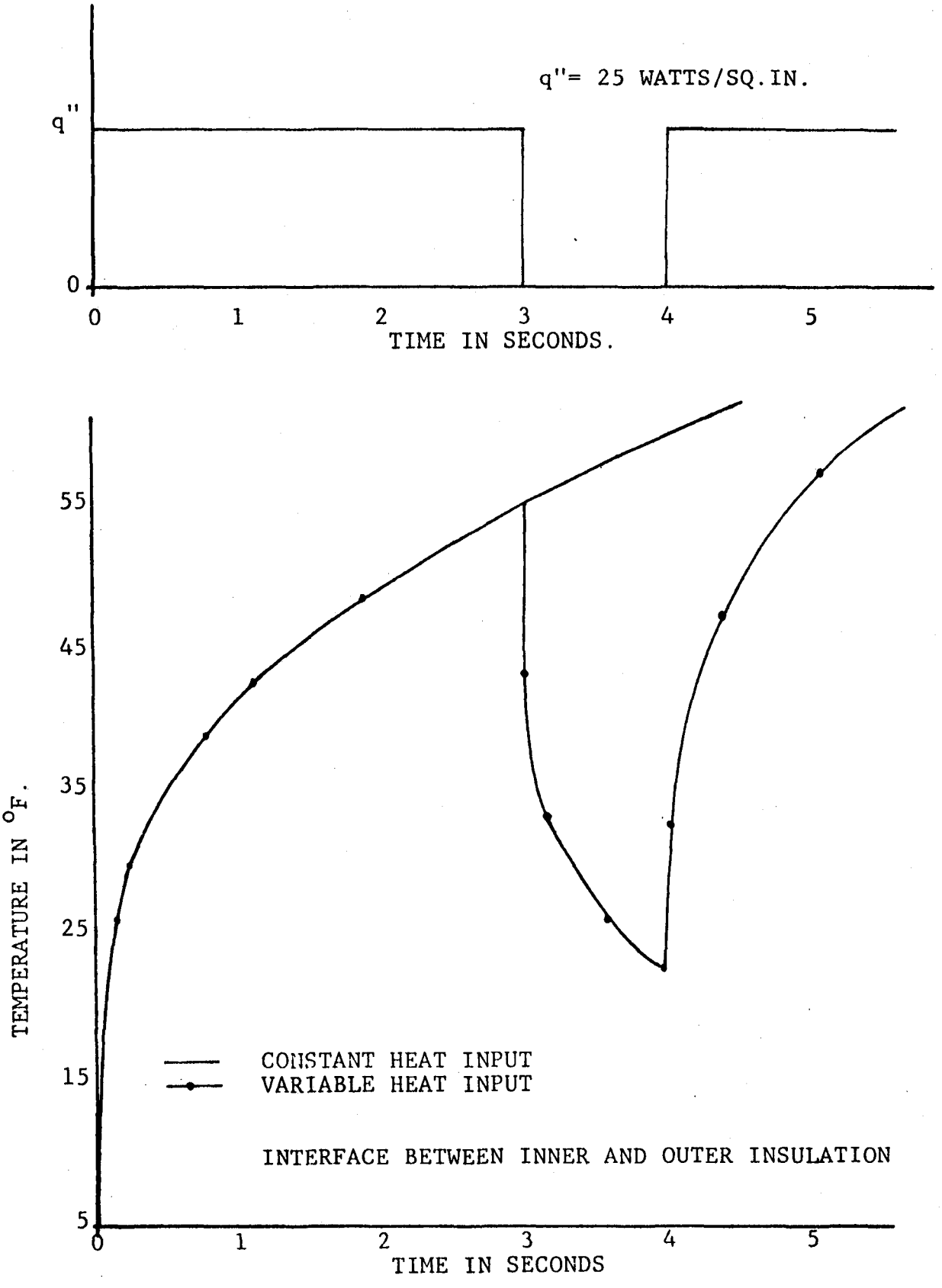

Figure 12b. Interfacial Temperature Response To Constant And Variable Point Heat Source

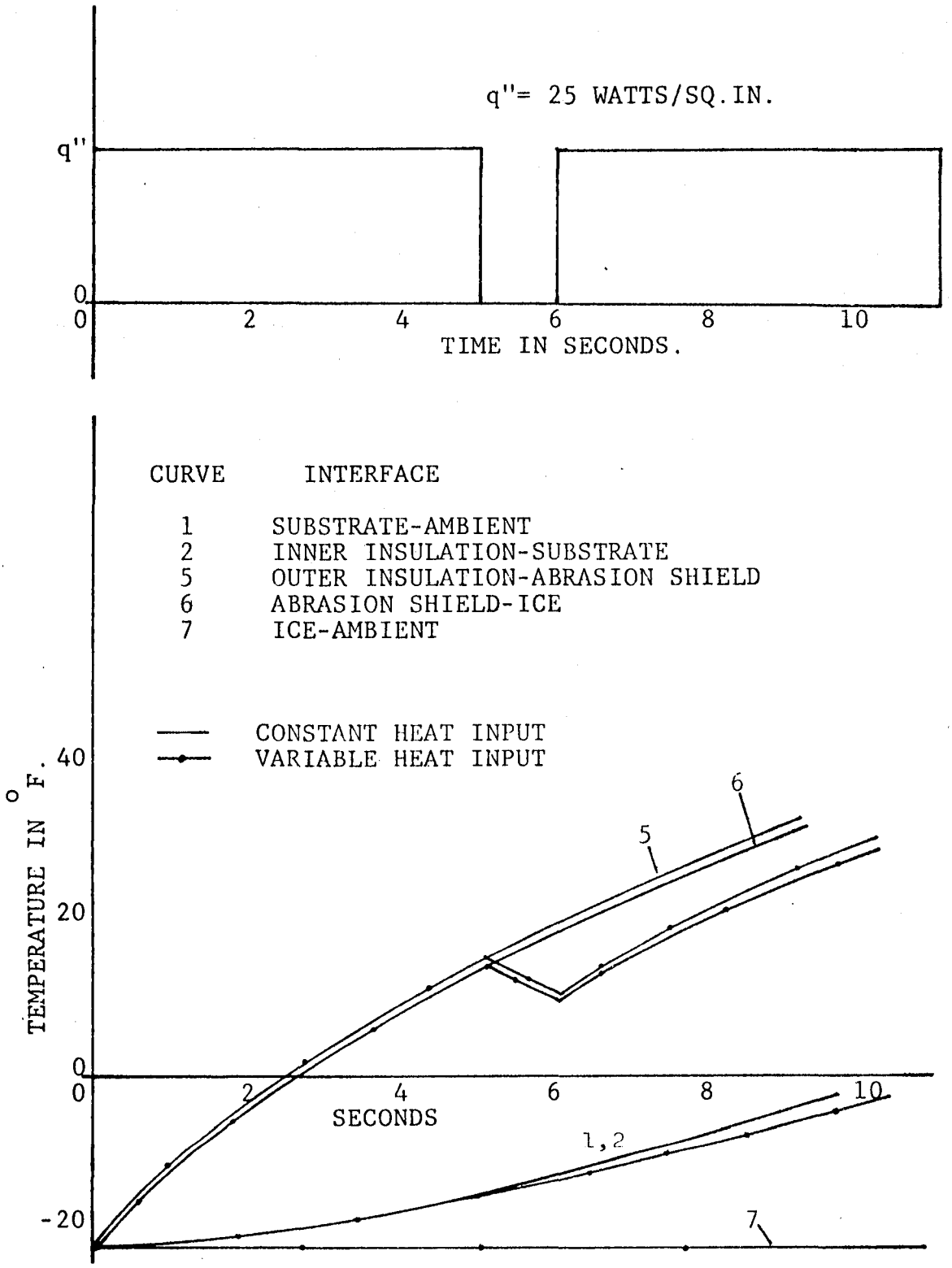

Figure 13a. Interfacial Temperature Response To Constant And Variable Finite Thickness Heat Source

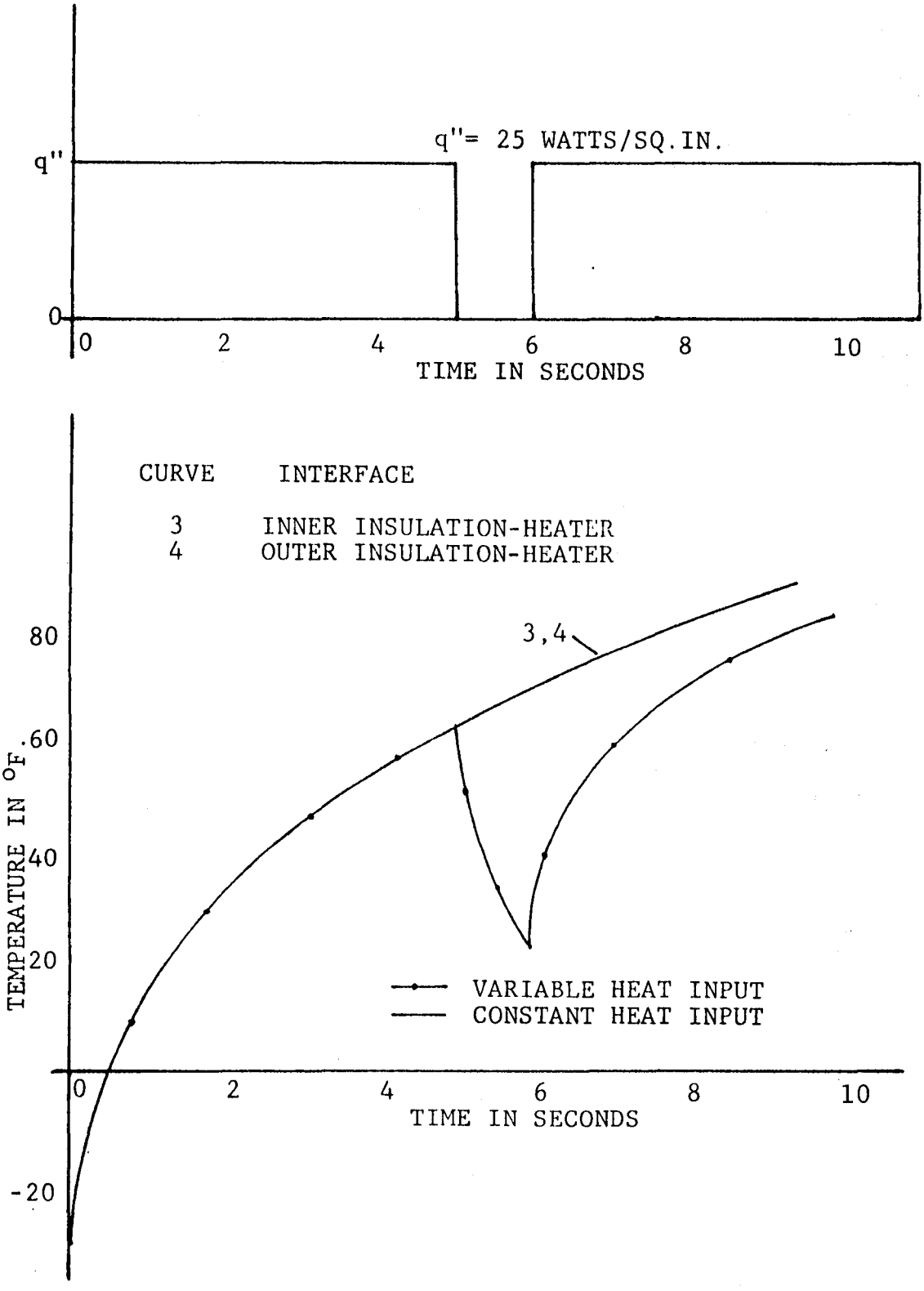

Figure 13b. Interfacial Temperature Response To Constant And Variable Finite Thickness Heat Source

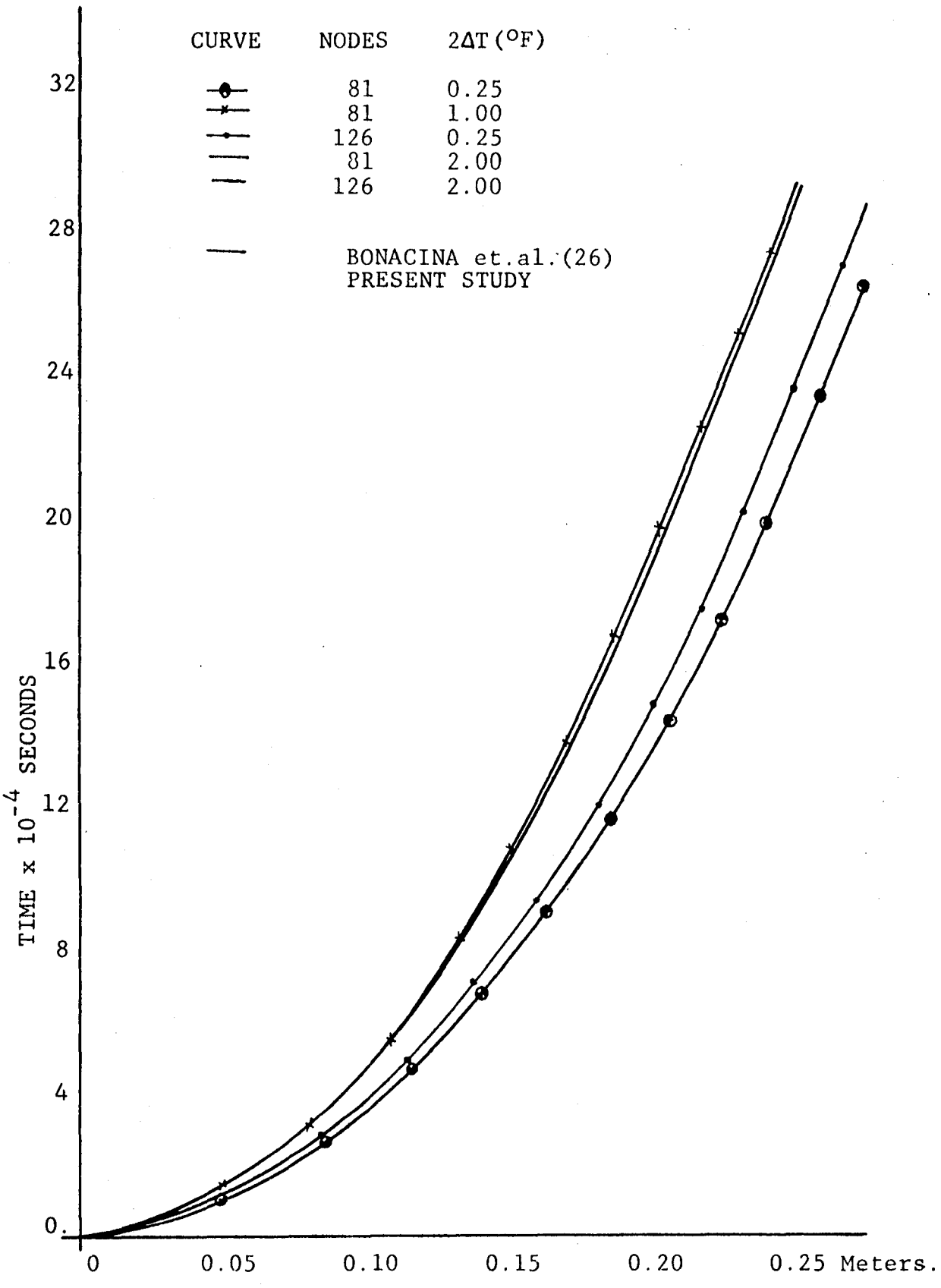

Figure 14. Interfacial Histories For One-Dimensional Water Solidification Problem

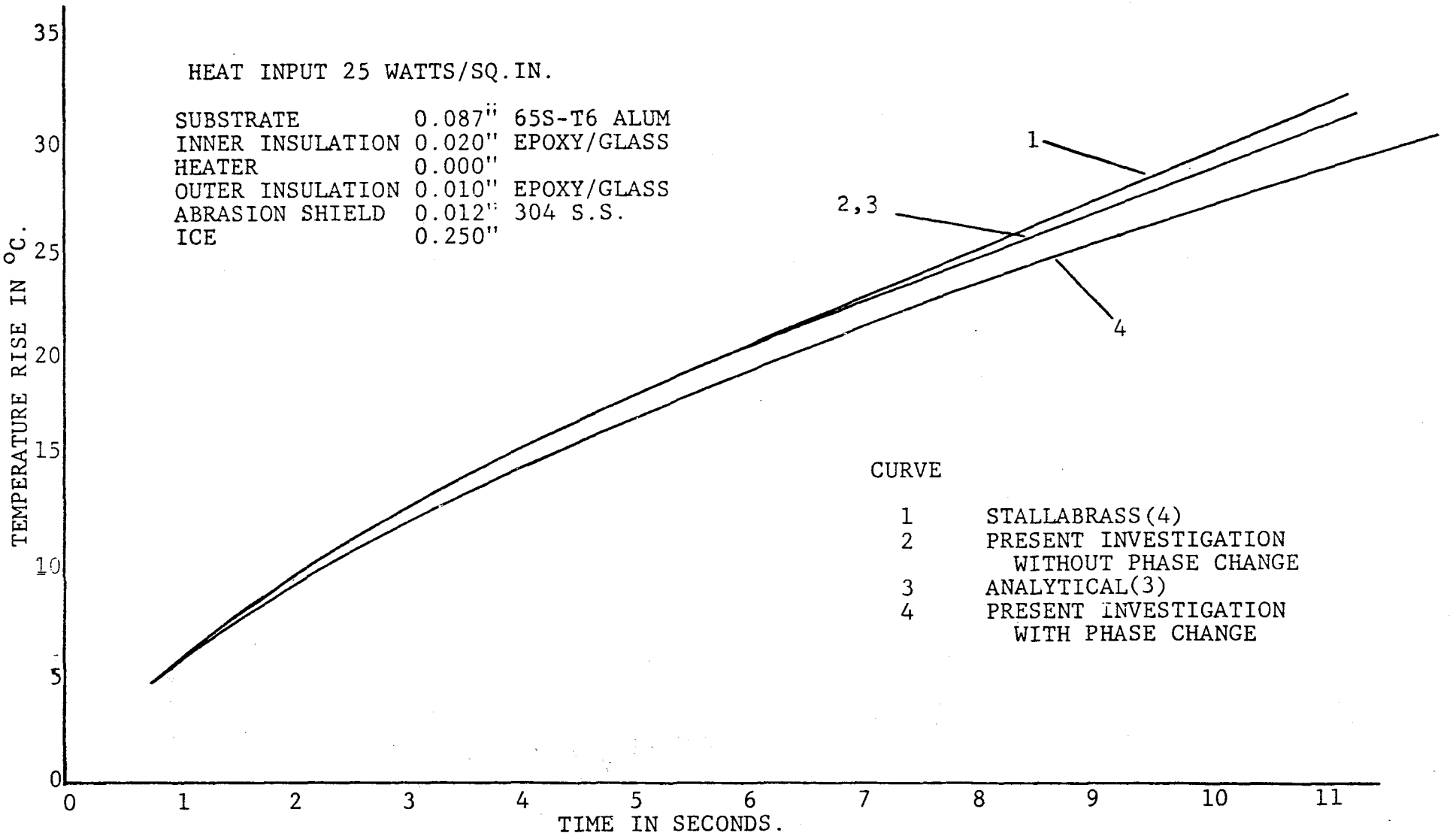

Figure 15a. Effect Of Phase Change On De-icing Time

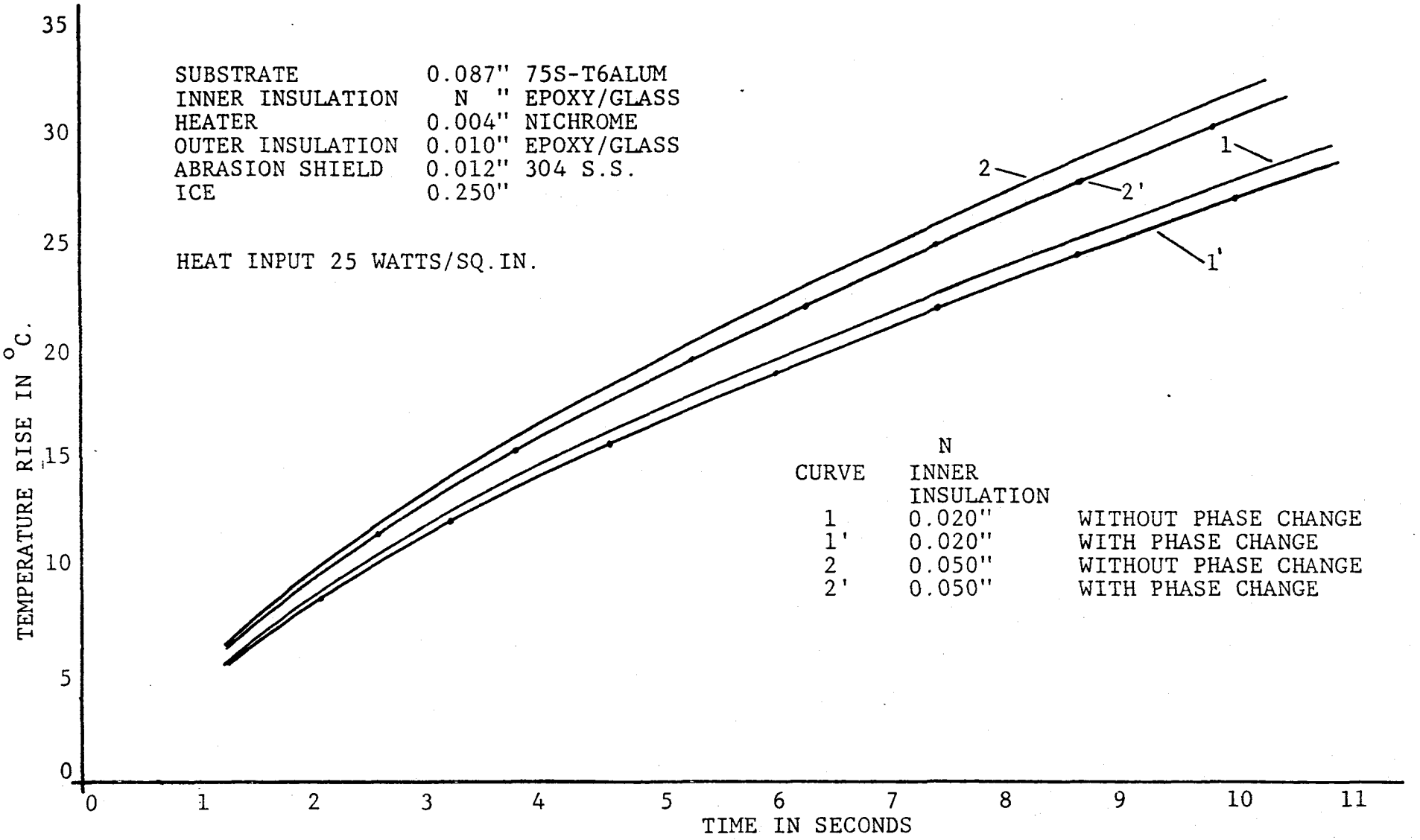

Figure 15b. Effect Of Phase Change On De-icing Time

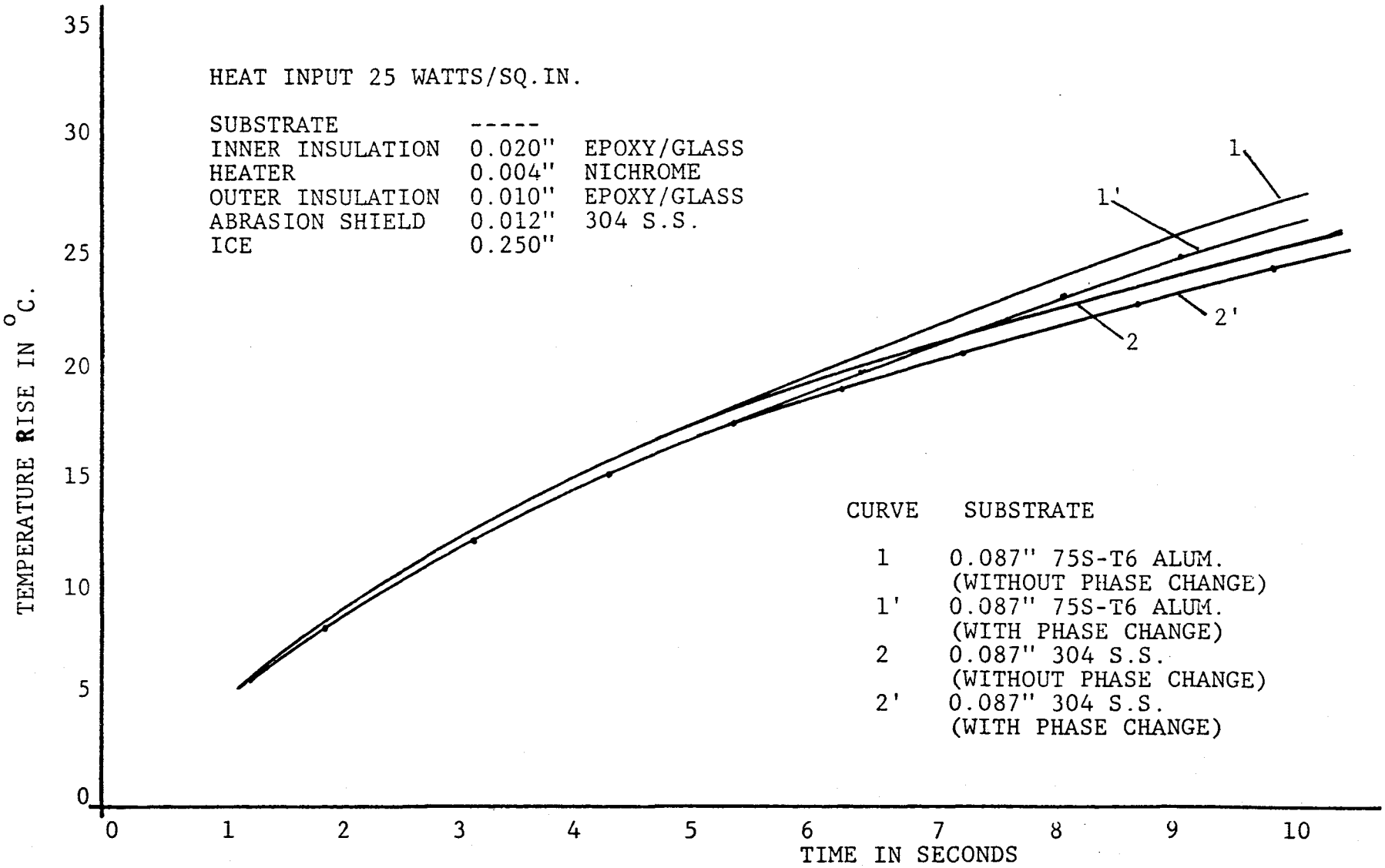

Figure 15c. Effect Of Phase Change On De-icing Time

APPENDIX I

COMPLETE PROGRAM LISTING

NUMERICAL SIMULATION OF ONE-DIMENSIONAL HEAT TRANSFER
IN COMPOSITE BODIES WITH PHASE CHANGE.

THIS PROGRAM CAN CALCULATE THE TEMPERATURE PROFILE IN A COMPOSITE SLAB WHICH HAS CONVECTIVE,CONSTANT TEMPERATURE OR MIXED BOUNDARY CONDITIONS.

THE PROGRAM CAN ALSO BE USED FOR COMPOSITE BODY PROBLEMS WITH CONSTANT OR VARIABLE HEAT SOURCES.

A,B,C,D	= TRIDIAGONAL MATRIX CONSTANTS.
AK	= THERMAL CONDUCTIVITIES OF LAYERS.
ALP	= THERMAL DIFFUSIVITIES OF LAYERS.
AKL	= THERMAL CONDUCTIVITY OF WATER.
ALPL	= THERMAL DIFFUSIVITY OF WATER.
CA	= CONSTANT.
CPS,CPL	= SPECIFIC HEAT OF ICE AND WATER PER UNIT VOLUME.
DTAUI	= INITIAL TIME STEP
DTAUM	= INTERMEDIATE TIME STEP
DTAUF	= FINAL TIME STEP
DX	= SPACING BETWEEN NODES.
EL	= LENGTH OF EACH LAYER.
HEAD	= HEADINGS.
H1	= HEAT TRANSFER COEFF. AT LOWER BOUNDARY.
H2	= HEAT TRANSFER COEFF. AT UPPER BOUNDARY.
HLAM	= LATENT HEAT OF ICE.
IBC1	= 1, IMPLIES TEMPERATURE IS CONSTANT AT X=0.
IBC1	= 2, IMPLIES CONVECTIVE HEAT TRANSFER AT X=0.
IBC2	= 1, IMPLIES TEMPERATURE IS CONSTANT AT X=1.
IBC2	= 2, IMPLIES CONVECTIVE HEAT TRANSFER AT X=1.
ICOUNT	= COUNTER ON TIME STEP.
IFREQ	= NUMBER OF TIME STEPS BETWEEN SUCCESSIVE PRINTING OF THE TEMPERATURE PROFILE.
IG	= 1, IMPLIES PHASE CHANGE IN ICE LAYER IS NOT CONSIDERED.

```
IG          = 2, IMPLIES PHASE CHANGE IN ICE LAYER IS
                                                    CONSIDERED
IH          = 1, IMPLIES NO HEAT SOURCE.
IH          = 2, IMPLIES POINT HEAT SOURCE.
IH          = 3, IMPLIES HEAT GENERATION WITHIN SLAB.
IHQ         = 1, IMPLIES CONSTANT HEAT SOURCE.
IHQ         = 2, IMPLIES VARIABLE HEAT SOURCE.
IJ          = SLAB WITHIN WHICH HEAT GENERATION OCCURS.
INTIME      = NUMBER OF TIME STEPS FOR WHICH INITIAL TIME
                                                STEP IS USED.
IMTIME      = NUMBER OF TIME STEPS FOR WHICH INTERMEDIATE
                                            TIME STEP IS USED.
M           = NUMBER OF NODES IN SLAB.
MM          = INTERFACE NODE NUMBERS.
N           = NUMBER OF LAYERS IN SLAB.
N1          = LOWER SLAB NUMBER FOR POINT HEAT SOURCE.
N2          = UPPER SLAB NUMBER FOR POINT HEAT SOURCE.
NO          = NUMBER OF NODES IN EACH LAYER.
NO1         = LOWER NODE NUMBER FOR FINITE THICKNESS HEATER.
NO2         = UPPER NODE NUMBER FOR FINITE THICKNESS HEATER.
NODE        = NODE AT WHICH POINT HEAT SOURCE IS APPLIED.
Q           = POINT HEAT SOURCE  WATTS/IN*IN.
Q2          = VOLUMETRIC HEAT SOURCE WATTS/IN*IN*IN.
QHEAT       = FUNCTION PROGRAM FOR VARIABLE HEAT INPUT.
QV          = STEP INPUT FOR VARIABLE HEAT SOURCE.
T           = NON-DIMENSIONAL TEMPERATURE.
TDIFF       = HALF PHASE CHANGE TEMPERATURE INTERVAL.
TE          = TEMPERATURE.
TG1         = AMBIENT TEMPERATURE AT LOWER BOUNDARY OF SLAB.
TG2         = AMBIENT TEMPERATURE AT UPPER BOUNDARY OF SLAB.
TIN         = INITIAL TEMPERATURE IN SLAB.
TLEN        = TOTAL LENGTH OF SLAB.
TMAX        = ICE-ABRASION SHIELD INTERFACE TEMPERATURE.
TOFF        = OFF TIME OF STEP HEAT INPUT.
TON         = ON TIME OF STEP HEAT INPUT.
TPHAS       = TEMPERATURE AT WHICH PHASE CHANGE OCCURS.
```

```
C       TR              = NON-DIMENSIONAL TEMPERATURE AT PREVIOUS
C       TREF            = REFERENCE TEMPERATURE.
C       TRIDAG          = SUBROUTINE TO SOLVE TRIDIAGNOL MATRIX.
C       TX0             = CONSTANT TEMPERATURE AT LOWER SLAB BOUNDARY.
C       TX1             = CONSTANT TEMPERATURE AT UPPER SLAB BOUNDARY.
C
      DATA IN/5/,IO/6/
      DIMENSION HEAD(40,80)
      DIMENSION A(100),B(100),C(100),D(100),T(200,100),TR(100),TE(100)
      DIMENSION ALP(6),CA(6),NO(6),MM(6),DX(6),AK(6),EL(6)
C
      INPUT  DATA
C
      DO 300 I=1,18
      READ(IN,100)(HEAD(I,J),J=1,80)
  300 CONTINUE
      READ(IN,101)N,M,TLEN
C
      DO 10 I=1,100
      A(I)=0.
      B(I)=0.
      C(I)=0.
      D(I)=0.
      TE(I)=0.
      TR(I)=0.
      DO 11 J=1,200
      T(J,I)=0.
   11 CONTINUE
   10 CONTINUE
      DO 12 K=1,N
      ALP(K)=0.
      AK(K)=0.
      EL(K)=0.
      DX(K)=0.
      CA(K)=0.
```

```
      NO(K)=0
      MM(K)=0
   12 CONTINUE

      INPUT DATA

      DO 301 I=19,22
  301 READ(IN,100)(HEAD(I,J),J=1,80)
      DO 13 K=1,N
      READ(IN,102) NO(K),EL(K),AK(K),ALP(K)
   13 CONTINUE
      DO 302 I=23,25
  302 READ(IN,100)(HEAD(I,J),J=1,80)
      READ(IN,103)IH,NODE,N1,N2
      READ(IN,104)IJ,NO1,NO2,THQ
      READ(IN,105)Q,TON,TOFF,QV
      DO 303 I=26,28
  303 READ(IN,100)(HEAD(I,J),J=1,80)
      READ(IN,106)IBC1,IBC2
      READ(IN,116)TX0,TX1
      READ(IN,107)TG1,H1,TG2,H2
      READ(IN,108)TIN,TREF
      DO 304 I=29,31
  304 READ(IN,100)(HEAD(I,J),J=1,80)
      READ(IN,109)IG,HLAM,ALPL,AKL,CPL,CPS
      READ(IN,110)TPHAS,TDIFF
      DO 305 I=32,34
  305 READ(IN,100)(HEAD(I,J),J=1,80)
      READ(IN,111)DTAUI,INSTEP,DTAUM,IMSTEP
      READ(IN,112)DTAUF,IFREQ,TMAX
      DO 315 I=35,40
  315 READ(IN,100)(HEAD(I,J),J=1,80)

       PRINT THE DATA

      DO 306 I=1,18
```

```
306 WRITE(IO,900)(HEAD(I,J),J=1,80)
    WRITE(IO,200)N,M,TLEN
    DO 307 I=19,22
307 WRITE(IO,900)(HEAD(I,J),J=1,80)
    DO 14 K=1,N
    WRITE(IO,102)NO(K),EL(K),AK(K),ALP(K)
 14 CONTINUE
    DO 308 I=23,25
308 WRITE(IO,900)(HEAD(I,J),J=1,80)
    IF(IH.EQ.1) GO TO 60
    IF(IH.EQ.2) GO TO 61
    WRITE(IO,201)IJ,NO1,NO2
    GO TO 62
 60 WRITE(IO,202)
    GO TO 62
 61 WRITE(IO,203)NODE,N1,N2
 62 IF(IHQ.EQ.1)WRITE(IO,204)Q
    IF(IHQ.EQ.2)WRITE(IO,224)TON,TOFF,QV
    DO 309 I=26,28
309 WRITE(IO,900)(HEAD(I,J),J=1,80)
    IF(IBC1.EQ.2) GO TO 63
    WRITE(IO,205)TX0
    GO TO 64
 63 WRITE(IO,206)TG1,H1
 64 IF(IBC2.EQ.2) GO TO 65
    WRITE(IO,207)TX1
    GO TO 66
 65 WRITE(IO,208)TG2,H2
 66 WRITE(IO,209)TIN,TREF
    WRITE(IO,900)(HEAD(26,J),J=1,80)
    IF(IG.EQ.1)GO TO 67
    WRITE(IO,210)
    WRITE(IO,900)(HEAD(29,J),J=1,80)
    WRITE(IO,900)(HEAD(28,J),J=1,80)
    WRITE(IO,900)(HEAD(30,J),J=1,80)
    WRITE(IO,900)(HEAD(31,J),J=1,80)
```

```
      WRITE(IO,211)HLAM,AKL,ALPL,CPL,CPS
      WRITE(IO,212)TPHAS,TDIFF
      GO TO 68
   67 WRITE(IO,213)
   68 WRITE(IO,900)(HEAD(26,J),J=1,80)
      DO 310 I=32,34
  310 WRITE(IO,900)(HEAD(I,J),J=1,80)
      WRITE(IO,218)DTAUI,INSTEP,DTAUM,IMSTEP
      WRITE(IO,214)DTAUF,IFREQ,TMAX
      WRITE(IO,900)(HEAD(1,J),J=1,80)
      WRITE(IO,217)
      WRITE(IO,900)(HEAD(16,J),J=1,80)
      WRITE(IO,900)(HEAD(1,J),J=1,80)

       INITIAL CONDITIONS

      FDIST=TIN/TREF
      G1TIME=TG2/TREF
      G0TIME=TG1/TREF
      X1TIME=TX1/TREF
      X0TIME=TX0/TREF
      TLEN=TLEN/12.
      DO 30 J=1,N
   30 EL(J)=EL(J)/12.
      TON=TON/3600.
      TOFF=TOFF/3600.
      DTAUI=DTAUI/3600.
      DTAUM=DTAUM/3600.
      DTAUF=DTAUF/3600.

      INTERFACE  NODE  NUMBERING

      MM(1)=NO(1)
      DO 16 L=2,N
      MM(L)=MM(L-1)+NO(L)-1
   16 CONTINUE
```

```
      PRINT THE INITIAL TEMPERATURE PROFILE

      ICOUNT=1
      DO 19 J=1,M
      FLOAT J=J
   19 T(ICOUNT,J)=FDIST
      TAU=0.
      WRITE(IO,215) TAU
      DO 31 I=1,M
   31 TE(I)=T(ICOUNT,I)*TREF
      WRITE(IO,216)(TE(I),I=1,M)

   88 LCOUNT=ICOUNT
      ICOUNT=LCOUNT+1
      IF(ICOUNT.LE.INSTEP)DTAU=DTAUI
      ITSTEP=INSTEP+IMSTEP
      IF((ICOUNT.LE.ITSTEP).AND.(ICOUNT.GT.INSTEP))DTAU=DTAUM
      IF(ICOUNT.GT.ITSTEP)DTAU=DTAUF
      MCL=200
      IF(ICOUNT.GT.MCL) GO TO 999
      TAU=TAU+DTAU

      CALCULATION OF CONSTANTS

      DO 15 I=1,N
      DX(I)=EL(I)/(TLEN*(NO(I)-1))
   15 CA(I)=(ALP(I)*DTAU)/(DX(I)*DX(I)*TLEN*TLEN)

      CALCULATION OF THE TRIDIAGNOL CONSTANTS

      IF(N.NE.1) GO TO 32
      DO 29 J=1,M
      A(J)=1.
      B(J)=-2.*(1.+1./CA(1))
   29 C(J)=1.
```

```
      GO TO 34
   32 LIST=1
      NEW=N-1
      DO 17 K=1,NEW
      NN=MM(K)
      B(NN)=-1.*((1.+1./CA(K))+((AK(K+1)*DX(K))/
     1(AK(K)*DX(K+1)))*(1.+1./CA(K+1)))
      C(NN)=(AK(K+1)*DX(K))/(AK(K)*DX(K+1))
      A(NN)=1.
      NNEW=NN-1
      DO 18 J=LIST,NNEW
      A(J)=1.
      B(J)=-2.*(1.+1./CA(K))
      C(J)=1.
   18 CONTINUE
      LIST=NN+1
   17 CONTINUE

      ACCOUNTING FOR PHASE CHANGE IN ICE LAYER

   34 IF(IG.EQ.1) GO TO 40
      THETA=TDIFF/TREF
      CSTAR=((CPS+CPL)/2.)+HLAM/(2.*TREF*THETA)
      CONST1=(TLEN*TLEN*DX(N)*DX(N))/(ALP(N)*DTAU)
      CONST2=(TLEN*TLEN*DX(N)*DX(N))/(ALPL*DTAU)
      CONST3=2.*TLEN*TLEN*DX(N)*DX(N)*CSTAR/DTAU
      THETA1=(TPHAS/TREF)+THETA
      THETA2=(TPHAS/TREF)-THETA
      TKK1=(AKL-AK(N))/(2.*THETA)

      ACCOUNTING FOR PHASE CHANGE IN THE ICE LAYER

   40 IF(N.EQ.1) GO TO 35
      IF(IG.EQ.1)GO TO 42
      LUST=LIST-1
```

```
      CALCULATION OF THERMAL CONDUCTIVITIES AND TEMPERATURES
         AT INTERMEDIATE TIME STEPS FOR "MUSHY" REGION.

      DO 20 J=LUST,M
      IF(J.EQ.LUST) GO TO 401
      IF(T(LCOUNT,J).GT.THETA1) GO TO 43
      IF(T(LCOUNT,J).LT.THETA2) GO TO 44

        TEMPERATURE AND THERMAL CONDUCTIVITY AT NODE I FOR AN
                INTERMEDIATE TIME STEP.

  401 TKMIN1=AK(N)+TKK1*(((T(LCOUNT,J)+T(LCOUNT,J-1))/2.)
     1-((TPHAS/TREF)-THETA))
      IF(TKMIN1.LT.AKL)TKMIN1=AKL
      IF(TKMIN1.GT.AK(N))TKMIN1=AK(N)
      T(LCOUNT,M+1)=G1TIME
      T(LCOUNT,M+2)=G1TIME
      PLUSK1=AK(N)+TKK1*(((T(LCOUNT,J)+T(LCOUNT,J+1))/2.)
     1-((TPHAS/TREF)-THETA))
      IF(PLUSK1.LT.AKL)PLUSK1=AKL
      IF(PLUSK1.GT.AK(N))PLUSK1=AK(N)
      TEMP1=T(LCOUNT,J)+(DTAU/(2.*CSTAR*TLEN*TLEN*DX(N)*DX(N)))
     1*((PLUSK1*(T(LCOUNT,J+1)-T(LCOUNT,J))-TKMIN1*(T(LCOUNT,J))
     2-T(LCOUNT,J-1)))

        TEMPERATURE AND THERMAL CONDUCTIVITY AT NODE I+1 FOR
                INTERMEDIATE TIME STEP.

      TKMIN2=AK(N)+TKK1*(((T(LCOUNT,J)+T(LCOUNT,J+1))/2.)
     1-((TPHAS/TREF)-THETA))
      IF(TKMIN2.LT.AKL)TKMIN2=AKL
      IF(TKMIN2.GT.AK(N))TKMIN2=AK(N)
      PLUSK2=AK(N)+TKK1*(((T(LCOUNT,J+2)+T(LCOUNT,J+1))/2.)
     1-((TPHAS/TREF)-THETA))
      IF(PLUSK2.LT.AKL)PLUSK=AKL
      IF(PLUSK2.GT.AK(N))PLUSK2=AK(N)
```

```
 TEMP2=T(LCOUNT,J+1)+(DTAU/(2.*CSTAR*TLEN*TLEN*DX(N)*DX(N)))
1*((PLUSK2*(T(LCOUNT,J+2)-T(LCOUNT,J+1))-TKMIN2*(T(LCOUNT,J+1))
2-T(LCOUNT,J)))
```

TEMPERATURE AND THERMAL CONDUCTIVITY AT NODE I-1 FOR INTERMEDIATE TIME STEP.

```
 TKMIN3=AK(N)+TKK1*(((T(LCOUNT,J-2)+T(LCOUNT,J-1))/2.)
1-((TPHAS/TREF)-THETA))
 IF(TKMIN3.LT.AKL)TKMIN3=AKL
 IF(TKMIN3.GT.AK(N))TKMIN3=AK(N)
 PLUSK3=AK(N)+TKK1*(((T(LCOUNT,J)+T(LCOUNT,J-1))/2.)
1-((TPHAS/TREF)-THETA))
 IF(PLUSK3.LT.AKL)PLUSK3=AKL
 IF(PLUSK3.GT.AK(N))PLUSK3=AK(N)
 TEMP3=T(LCOUNT,J-1)+(DTAU/(2.*CSTAR*TLEN*TLEN*DX(N)*DX(N)))
1*((PLUSK3*(T(LCOUNT,J)-T(LCOUNT,J-1))-TKMIN3*(T(LCOUNT,J-1))
2-T(LCOUNT,J-2)))
```

CALCULATION OF THERMAL CONDUCTIVITY FOR "MUSHY" REGION.

```
 TKMIN=AK(N)+TKK1*(((TEMP1+TEMP3)/2.)
1-((TPHAS/TREF)-THETA))
 IF(TKMIN.LT.AKL)TKMIN=AKL
 IF(TKMIN.GT.AK(N))TKMIN=AK(N)
 PLUSK=AK(N)+TKK1*(((TEMP1+TEMP2)/2.)
1-((TPHAS/TREF)-THETA))
 IF(PLUSK.LT.AKL)PLUSK=AKL
 IF(PLUSK.GT.AK(N))PLUSK=AK(N)
```

THERMAL CONDUCTIVITY AT THE ICE-AMBIENT BOUNDARY

```
 IF(J.NE.M)GO TO 403
 PKB=AK(N)+TKK1*(TEMP1-((TPHAS/TREF)-THETA))
 IF(PKB.LT.AKL)PKB=AKL
 IF(PKB.GT.AK(N))PKB=AK(N)
```

```
      IF(J.EQ.M)GO TO 45

        THERMAL CONDUCTIVITY OF "MUSHY" REGION AT ICE-ABRASION
                                          SHIELD INTERFACE.*

  403 IF(J.NE.LUST)GO TO 402
      PKINC=AK(N)+TKK1*(TEMP1-((TPHAS/TREF)-THETA))
      IF(PKINC.LT.AKL)PKINC=AKL
      IF(PKINC.GT.AK(N))PKINC=AK(N)
      TKINC2=TKMIN
      PKINC2=PLUSK
      GO TO 20

        APPLYING HEAT EQUATION FOR "MUSHY" REGION.

  402 A(J)=TKMIN
      B(J)=-1.*(TKMIN+PLUSK+CONST3)
      C(J)=PLUSK
      D(J)=-T(LCOUNT,J-1)*TKMIN-PLUSK*T(LCOUNT,J+1)+T(LCOUNT,J)
     1*(TKMIN+PLUSK-CONST3)
      GO TO 20

        APPLYING HEAT EQUATION FOR LIQUID REGION.

   43 IF(J.EQ.M)GO TO 45
      A(J)=1.
      B(J)=-2.*(1.+CONST2)
      C(J)=1.
      D(J)=-T(LCOUNT,J+1)-T(LCOUNT,J-1)+T(LCOUNT,J)
     1*2.*(1.-1.*CONST2)
      GO TO 20

        APPLYING HEAT EQUATION FOR SOLID REGION.

   44 IF(J.EQ.M)GO TO 45
      A(J)=1.
```

```
      B(J)=-2.*(1.+1./CA(N))
      C(J)=1.
      D(J)=-T(LCOUNT,J+1)-T(LCOUNT,J-1)+T(LCOUNT,J)
     1*2.*(1.-1./CA(N))
   20 CONTINUE
      GO TO 45

        CALCULATION OF CONSTANT FOR SINGLE SLAB.

   42 A(M)=1.
      C(M)=1.
      MEW=M-1
      DO 33 J=LIST,MEW
      A(J)=1.
      C(J)=1.
      B(J)=-2.*(1.+1./CA(N))
      D(J)=-T(LCOUNT,J+1)-T(LCOUNT,J-1)+T(LCOUNT,J)
     1*2.*(1.-1./CA(N))
   33 CONTINUE
   45 LA=2
      A(M)=1.
      C(M)=0.

        CALCULATIONS OF THE INTERFACE CONSTANTS

      NEW=N-1
      DO 21 K=1,NEW
      NN=MM(K)
      D(NN)=-T(LCOUNT,NN+1)*((AK(K+1)*DX(K))/(AK(K)*DX(K+1)))
     1+((1.-1./CA(K))+((AK(K+1)*DX(K))/(AK(K)*DX(K+1)))
     2*(1.-1./CA(K+1)))*T(LCOUNT,NN)-T(LCOUNT,NN-1)
      NNEW=NN-1
      DO 22 J=LA,NNEW
      D(J)=-T(LCOUNT,J+1)-T(LCOUNT,J-1)+T(LCOUNT,J)
     1*(2.-2./CA(K))
   22 CONTINUE
```

```
56 D(M)=-T(LCOUNT,M-1)-(2.*TLEN*H2*DX(N)/AK(N))*G1TIME
  1+((1.-1./CA(N))+(H2*TLEN*DX(N)/AK(N)))*T(LCOUNT,M)
   B(M)=-(1.+1./CA(N))-(H2*TLEN*DX(N))/AK(N)
   A(M)=1.
   GO TO 49
48 MIN=M-1
   D(MIN)=D(MIN)-X1TIME*C(MIN)
   T(ICOUNT,M)=X1TIME

  CALCULATION AT THE ICE-ABRASION SHIELD INTERFACE

49 INC=MM(N-1)
   IF(IG.EQ.1) GO TO 50
   IF(T(LCOUNT,INC).LT.THETA2)GO TO 50
   IF(T(LCOUNT,INC).GT.THETA1) GO TO 51
   DUCT=DX(N-1)*PKINC/(2.*TKINC2*DX(N)*AK(N-1))
   A(INC)=1.
   B(INC)=-(1.+1./CA(N-1))-(DUCT*(TKINC2+PKINC2+CONST3))
   C(INC)=DUCT*(TKINC2+PKINC2)
   D(INC)=-DUCT*(TKINC2+PKINC2)*T(LCOUNT,INC+1)-T(LCOUNT,INC-1)
  1+((1.-1./CA(N-1))+(TKINC2+PKINC2-CONST3)*DUCT)*T(LCOUNT,INC)
   GO TO 50
51 A(INC)=1.
   B(INC)=-1.*((1.+1./CA(N-1))+((AKL*DX(N-1))/(AK(N-1)*DX(N)))
  1*(1.+(ALP(N)/(CA(N)*ALPL))))
   C(INC)=(AKL*DX(N-1))/(AK(N-1)*DX(N))
   D(INC)=-(AKL*DX(N-1)/(AK(N-1)*DX(N)))*T(LCOUNT,INC+1)
  1-T(LCOUNT,INC-1)+T(LCOUNT,INC)*((1.-1./CA(N-1))+
  2(1.-(ALP(N)/(ALPL*CA(N))))*(AKL*DX(N-1)/(AK(N-1)*DX(N))))

    HEAT TERM INCLUSION

50 IF(IHQ.EQ.1)Q1=Q
   IF(IHQ.EQ.2)Q1=QHEAT(TAU,TON,TOFF,QV)
   IF(IH.EQ.1) GO TO 52
   IF(IH.EQ.2) GO TO 53
```

```
      LA=NN+1
   21 CONTINUE

      ACCOUNTING FOR BOUNDARY CONDITIONS

   35 IF(N.NE.1) GO TO 36
      MEW=M-1
      DO 37 I=2,MEW
   37 D(I)=-T(LCOUNT,I+1)-T(LCOUNT,1-1)+T(LCOUNT,I)
     1*(2.-2./CA(1))
   36 IF(IBC1.EQ.1) GO TO 46
      D(1)=-T(LCOUNT,2)-(2.*H1*TLEN*DX(1)/AK(1))*GOTIME
     1+((1.-1./CA(1))+(H1*TLEN*DX(1)/AK(1)))*T(LCOUNT,1)
      B(1)=-(1.+1./CA(1))-(H1*TLEN*DX(1)/AK(1))
      C(1)=1.
      GO TO 47
   46 D(2)=D(2)-XOTIME
      T(ICOUNT,1)=XOTIME
   47 IF(IBC2.EQ.1) GO TO 48
      IF(IG.EQ.1)GO TO 56

        ACCOUNTING FOR PHASE CHANGE AT UPPER BOUNDARY

      IF(T(LCOUNT,M).LT.THETA2)GO TO 56
      IF(T(LCOUNT,M).GT.THETA1)GO TO 57
      A(M)=TKMIN+PLUSK
      B(M)=-((PLUSK+TKMIN+CONST3)+(2.*H2*TLEN*PLUSK*DX(N)/PKB))
      D(M)=-(TKMIN+PLUSK)*T(LCOUNT,M-1)-(4.*H2*TLEN*PLUSK*DX(N)*
     1G1TIME)/PKB+T(LCOUNT,M)*(PLUSK+TKMIN-CONST3+
     2(2.*H2*TLEN*PLUSK*DX(N)/PKB))
      GO TO 49
   57 D(M)=-T(LCOUNT,M-1)-(2.*TLEN*H2*DX(N)/AKL)*G1TIME
     1+((1.-(TLEN*TLEN*DX(N)*DX(N)/(ALPL*DTAU)))+(H2*TLEN*DX(N)/AKL))
     2*T(LCOUNT,M)
      B(M)=-1.-(TLEN*TLEN*DX(N)*DX(N)/(ALPL*DTAU))-(H2*TLEN*DX(N)/AKL)
      GO TO 49
```

```
      FINITE THICKNESS HEATER

      Q2=3.4121*144.*Q1/(TLEN*DX(IJ))
      HEAT=((DX(IJ)*TLEN)**2)*Q2/(TREF*AK(IJ))
      FACT1=AK(IJ)*DX(IJ-1)/(AK(IJ-1)*DX(IJ))
      FACT2=AK(IJ+1)*DX(IJ)/(AK(IJ)*DX(IJ+1))
      IF((NO2-NO1).GT.1)GO TO 54
      A(NO1)=1.
      C(NO1)=FACT1
      A(NO2)=1.
      C(NO2)=FACT2
      B(NO1)=-1.*((1.+1./CA(IJ-1))+FACT1*(1.+1./CA(IJ)))
      B(NO2)=-1.*((1.+1./CA(IJ))+FACT2*(1.+1./CA(IJ+1)))
   54 D(NO1)=-T(LCOUNT,NO1-1)-FACT1*T(LCOUNT,NO1+1)
     1+((1.-1./CA(IJ-1))+(1.-1./CA(IJ))*FACT1)*T(LCOUNT,NO1)-FACT1*HEAT
      D(NO2)=-T(LCOUNT,NO2-1)-FACT2*T(LCOUNT,NO2+1)-HEAT
     1+((1.-1./CA(IJ))+(1.-1./CA(IJ+1))*FACT2)*T(LCOUNT,NO2)
      IF((NO2-NO1).LE.1)GO TO 52
      NOW=NO1+1
      NNOW=NO2-1
      DO 55 IL=NOW,NNOW
   55 D(IL)=D(IL)-2.*HEAT
      GO TO 52

      POINT HEAT SOURCE

   53 D(NODE)=D(NODE)-(2.*TLEN*DX(N1)*Q1*3.4121*144.)/(TREF*AK(N1))

        SOLVING THE TRIDIAGNOL MATRIX

   52 IF((IBC1.EQ.2).AND.(IBC2.EQ.2))GO TO 94
      IF((IBC1.EQ.1).AND.(IBC2.EQ.1))GO TO 95
      IF((IBC1.EQ.2).AND.(IBC2.EQ.1))GO TO 96
      CALL TRIDAG(2,M,A,B,C,D,TR)
      TR(1)=XOTIME
```

```
      GO TO 97
   95 MIN=M-1
      CALL TRIDAG(2,MIN,A,B,C,D,TR)
      TR(1)=X0TIME
      TR(M)=X1TIME
      GO TO 97
   94 CALL TRIDAG(1,M,A,B,C,D,TR)
      GO TO 97
   96 MIN=M-1
      CALL TRIDAG(1,MIN,A,B,C,D,TR)
      TR(M)=X1TIME
   97 TMAX1=TMAX/TREF
      DO 23 J=1,M
      T(ICOUNT,J)=TR(J)
      TE(J)=TR(J)*TREF
   23 CONTINUE
      IF((ICOUNT/IFREQ)*IFREQ.NE.ICOUNT)GO TO 88
      MOVER2=INC
      TITAU=TAU*3600.
      WRITE(IO,215)TITAU
      WRITE(IO,216)(TE(I),I=1,M)
      WRITE(IO,900)(HEAD(1,J),J=1,80)
      WRITE(IO,900)(HEAD(35,J),J=1,80)
      WRITE(IO,900)(HEAD(1,J),J=1,80)
      JI=1
      NEW=N-1
      DO 24 L=1,NEW
      ID=35+L
      INT=MM(L)
      WRITE(IO,900)(HEAD(ID,JD),JD=1,80)
      WRITE(IO,216)(TE(I),I=JI,INT)
      JI=INT
   24 CONTINUE
      IF(T(ICOUNT,MOVER2).LE.TMAX1) GO TO 88
  100 FORMAT(80A1)
  900 FORMAT(' ',80A1)
```

```
   1F13.6,'DEG.F'// ' THE REFERENCE TEMPERATURE',20X,' TREF =',F13.6,
   2'DEG.F')
210 FORMAT(// ' THE PHASE CHANGE IN THE ICE LAYER IS CONSIDERED ')
211 FORMAT(/ ' LATENT HEAT OF ICE ',21X,' HLAM =',F13.6,'B.T.U./LB'/
   1' THERMAL CONDUCTIVITY OF WATER',12X,'AKL  =',F13.6,'B.T.U./HR.
   2FT.DEG.F'/ ' THERMAL DIFFUSIVITY OF WATER ',12X,'ALPL =',F13.6,
   3' FT.FT/HR.'/ ' SPECIFIC HEAT * DENSITY OF WATER ',8X,'CPL  =',
   4F13.6,'B.T.U./CU.FT.DEG.F'/ ' SPECIFIC HEAT * DENSITY OF ICE ',
   5,10X,'CPS  =',F13.6,'B.T.U./CU.FT.DEG.F')
212 FORMAT(/ ' PHASE CHANGE TEMPERATURE',24X,'TPHAS =',F13.6,'DEG.F'/
   1' HALF PHASE CHANGE TEMPERATURE INTERVAL          TDIFF=',F13.6,
   2'DEG.F')
213 FORMAT(// ' THE PHASE CHANGE IN THE ICE LAYER IS NOT CONSIDERED')
218 FORMAT(/ ' INITIAL TIME STEP',26X,'DTAUI =',F13.6,'SECS'/28X,
   1'FOR TIME STEPS INSTEP =',I3/ ' INTERMEDIATE TIME STEP',21X,
   2'DTAUM =',F13.6,'SECS'/28X,'FOR TIME STEPS IMSTEP =',I3)
214 FORMAT(/ ' FINAL TIME STEP',28X,'DTAUF =',F13.6,'SECS'/1X,
   1' FREQUENCY OF TIME STEP/PRINT OF OUTPUT',8X,'IFREQ =',I3/
   21X,' MAX. TEMP. AT ICE-ABRASION SHIELD INTERFACE',4X,
   3'TMAX =',F13.6,'DEG.F')
217 FORMAT(///28X,' TEMPERATURE PROFILE  IN  DEGREES F  ')
215 FORMAT(///35X,' TIME  TAU =',F15.6,' SECS')
216 FORMAT(/15X,5F13.5)
999 STOP
    END

    SUBROUTINE TRIDAG(IF,L,A,B,C,D,V)
    DIMENSION A(1),B(1),C(1),D(1),V(1),BETA(100),GAMMA(100)
    DO 10 I=1,100
    BETA(I)=0.
    GAMMA(I)=0.
 10 CONTINUE
    BETA(IF)=B(IF)
    GAMMA(IF)=D(IF)/BETA(IF)
    IFP1=IF+1
    DO 1 I=IFP1,L
```

```
101 FORMAT(54X,I3/54X,I3/54X,F12.6)
102 FORMAT(7X,I2,7X,F10.5,9X,F13.6,14X,F13.6)
103 FORMAT(53X,I3/53X,I3/53X,I3/53X,I3)
104 FORMAT(53X,I3/53X,I3/53X,I3/53X,I3)
105 FORMAT(53X,F11.5/53X,F11.5/53X,F11.5/53X,F11.5)
106 FORMAT(53X,I3/53X,I3)
116 FORMAT(46X,F13.6/46X,F13.6)
107 FORMAT(46X,F13.6/46X,F15.6/46X,F13.6/46X,F15.6)
108 FORMAT(46X,F13.6/46X,F13.6)
109 FORMAT(61X,I3/47X,F13.6/47X,F13.6/47X,F13.6/47X,F13.6/47X,F13.6)
110 FORMAT(47X,F13.6/47X,F13.6)
111 FORMAT(50X,F13.6/50X,I3/50X,F13.6/50X,I3)
112 FORMAT(50X,F13.6/50X,I3/50X,F13.6)
200 FORMAT(/ ' TOTAL NUMBER OF SLABS',31X,'N=',I3/ ' TOTAL NUMBER
   1 OF NODES',31X,'M=',I3/ ' TOTAL LENGTH OF COMPOSITE SLAB',
   219X,'TLEN=',F13.6,'INCHS')
201 FORMAT(' INTERNAL HEAT GENERATION IN SLAB NUMBER',9X,' IJ=',
   1I3/33X,'BETWEEN NODE    NO1=',I3/36X,'AND NODE     NO2=',I3)
202 FORMAT(//10X,'THERE  IS  NO  HEAT  SOURCE  PRESENT  ')
203 FORMAT(/ ' POINT HEAT SOURCE IS PRESENT AT',17X,'NODE=',I3/
   133X,'BETWEEN SLAB     N1=',I3/36X,'AND  SLAB     N2=',I3)
204 FORMAT(/ ' CONSTANT HEAT INPUT OF',28X,'Q =',F13.6,'WATTS/IN*IN')
224 FORMAT(/ ' ON-TIME FOR HEAT INPUT',27X,'TON=',F13.6,'SECS'/
   1' OFF-TIME FOR HEAT INPUT',25X,'TOFF=',F13.6,'SECS'/
   1' VARIABLE HEAT INPUT OF',28X,'QV=',F13.6,'WATTS/IN*IN')
205 FORMAT(// ' CONSTANT TEMPERATURE   AT  X=0',17X,' TX0=',F13.6,
   1' DEG.F')
206 FORMAT(// ' CONVECTION OCCURS      AT  X=0'/11X,'AMBIENT TEMPERAT
   1URE',5X,'TG1=',F13.6,'DEG.F'/11X,'HEAT TRANSFER COEFF.',5X,'H1=',
   2F15.6,'B.T.U/HR.FT.FT.DEG.F')
207 FORMAT(// ' CONSTANT TEMPERATURE   AT  X=1',17X,'TX1=',F13.6,
   1'DEG.F')
208 FORMAT(// ' CONVECTION OCCURS      AT  X=1'/11X,'AMBIENT TEMPERAT
   1URE',5X,'TG2=',F13.6,'DEG.F'/11X,'HEAT TRANSFER COEFF.',5X,'H2=',
   2F15.6,'B.T.U/HR.FT.FT.DEG.F')
209 FORMAT(/ ' THE INITIAL TEMPERATURE IN THE COMPOSITE SLAB  TIN =',
```

```
      BETA(I)=B(I)-A(I)*C(I-1)/BETA(I-1)
    1 GAMMA(I)=(D(I)-A(I)*GAMMA(I-1))/BETA(I)
      V(L)=GAMMA(L)
      LAST=L-IF
      DO 2 K=1,LAST
      I=L-K
    2 V(I)=GAMMA(I)-C(I)*V(I+1)/BETA(I)
      RETURN
      END
C
      FUNCTION QHEAT(TAU,TON,TOFF,QV)
      IN=IFIX(TAU/(TON+TOFF))
      IP=IN+1
      A =IN*(TON+TOFF)
      B =IN*TOFF+IP*TON
      C =IP*(TON+TOFF)
      QHEAT=Q
      IF((B.LT.TAU).AND.(TAU.LT.C))QHEAT=0.
      IF(TAU.EQ.TON)QHEAT=QV
      TTON=TON+TOFF
      IF(TAU.EQ.TTON)QHEAT=QV
      RETURN
      END
```

1. Report No.	2. Government Accession No.	3. Recipient's Catalog No.
NASA CR-165607		

4. Title and Subtitle	5. Report Date
NUMERICAL SIMULATION OF ONE-DIMENSIONAL HEAT TRANSFER IN COMPOSITE BODIES WITH PHASE CHANGE	March 1982
	6. Performing Organization Code

7. Author(s)	8. Performing Organization Report No.
Kenneth J. DeWitt and Gurudutt Baliga	None
	10. Work Unit No.

9. Performing Organization Name and Address	11. Contract or Grant No.
University of Toledo Department of Chemical Engineering Toledo, Ohio 43606	NAG 3-72
	13. Type of Report and Period Covered
12. Sponsoring Agency Name and Address	Contractor Report
National Aeronautics and Space Administration Washington, D.C. 20546	14. Sponsoring Agency Code
	505-44-12

15. Supplementary Notes

Final report. Project Manager, Robert J. Shaw, Propulsion Systems Division, NASA Lewis Research Center, Cleveland, Ohio 44135. Based on thesis submitted by Gurudutt Baliga as partial fulfillment of the requirements for the degree Master of Science to the University of Toledo, Toledo, Ohio in 1980.

16. Abstract

A numerical simulation is developed to investigate the one-dimensional heat transfer occurring in a system composed of a layered aircraft blade having an ice deposit on its surface. The finite-difference representation of the heat conduction equations is done using the Crank-Nicolson implicit finite-difference formulation. The simulation considers uniform or time-dependent heat sources, from heaters which can be either point sources or of finite thickness. For the icewater phase change, a numerical method which approximates the latent heat effect by a large heat capacity over a small temperature interval has been applied. The simulation describes the temperature profiles within the various layers of the de-icer pad, as well as the movement of the ice-water interface. The simulation could also be used to predict the one-dimensional temperature profiles in any composite slab having different boundary conditions.

17. Key Words (Suggested by Author(s))	18. Distribution Statement
Aircraft icing Electrothermal deicing One-dimensional, transient heat conduction	Unclassified - unlimited STAR Category 01

19. Security Classif. (of this report)	20. Security Classif. (of this page)	21. No. of Pages	22. Price*
Unclassified	Unclassified	88	

* For sale by the National Technical Information Service, Springfield, Virginia 22161